Stem Cell Reports
Article

ISSCR

OPEN ACCESS

Targeted Derivation of Organotypic Glucose- and GLP-1-Responsive β Cells Prior to Transplantation into Diabetic Recipients

Yaxi Zhu,[1,3] Jason M. Tonne,[1] Qian Liu,[2] Claire A. Schreiber,[1] Zhiguang Zhou,[3] Kuntol Rakshit,[4] Aleksey V. Matveyenko,[4,5] Andre Terzic,[5] Dennis Wigle,[5,6] Yogish C. Kudva,[7] and Yasuhiro Ikeda[1,5,8,*]

[1]Department of Molecular Medicine, Mayo Clinic, College of Medicine, 200 First Street SW, Rochester, MN 55905, USA
[2]Department of Orthopedics, The Second Xiangya Hospital, Central South University, Changsha, Hunan, China
[3]Institute of Metabolism and Endocrinology, The Second Xiangya Hospital, Key Laboratory of Diabetes Immunology, Ministry of Education, Central South University, National Clinical Research Center for Metabolic Diseases, Changsha, Hunan, China
[4]Department of Physiology and Biomedical Engineering, Mayo Clinic, Rochester, MN, USA
[5]Center for Regenerative Medicine, Mayo Clinic, Rochester, MN, USA
[6]Division of Thoracic Surgery, Mayo Clinic, Rochester, MN, USA
[7]Division of Endocrinology, Mayo Clinic, Rochester, MN, USA
[8]Present address: AstraZeneca, R&D, Antibody Discovery & Protein Engineering, One MedImmune Way, Gaithersburg, MD 20878, USA
*Correspondence: yasuhiro.ikeda@astrazeneca.com
https://doi.org/10.1016/j.stemcr.2019.07.006

SUMMARY

Generation of functional β cells from pluripotent sources would accelerate diagnostic and therapeutic applications for diabetes research and therapy. However, it has been challenging to generate competent β cells with dynamic insulin-secretory capacity to glucose and incretin stimulations. We introduced transcription factors, critical for β-cell development and function, in differentiating human induced pluripotent stem cells (PSCs) and assessed the impact on the functionality of derived β-cell (psBC) progeny. A perifusion system revealed stepwise transduction of the PDX1, NEUROG3, and MAFA triad (PNM) enabled *in vitro* generation of psBCs with glucose and GLP-1 responsiveness within 3 weeks. PNM transduction upregulated genes associated with glucose sensing, insulin secretion, and β-cell maturation. In recipient diabetic mice, PNM-transduced psBCs showed glucose-responsive insulin secretion as early as 1 week post transplantation. Thus, enhanced pre-emptive β-cell specification of PSCs by PNM drives generation of glucose- and incretin-responsive psBCs *in vitro*, offering a competent tissue-primed biotherapy.

INTRODUCTION

Diabetes affects more than 442 million adults worldwide (WHO, 2016), and this number is estimated to reach 642 million by 2040 (Ogurtsova et al., 2017). Whereas type 1 diabetes (T1D) results from autoimmune destruction of pancreatic β cells, type 2 diabetes (T2D) is caused by peripheral insulin resistance, β-cell dysfunction, and β-cell loss (Butler et al., 2003). Transplantation of stem cell-derived insulin-producing cells could provide a cell therapy option to restore β-cell loss or dysfunction in patients with diabetes (Holditch et al., 2014). Because of the capacity for unlimited self-renewal and pluripotent lineage specification, human pluripotent stem cells (PSCs) have been extensively studied for β-cell generation potential (Holditch et al., 2014). For the generation of β-like insulin-producing cells from PSCs guided differentiation protocols have been developed, which model the key stages of pancreatic development *in vitro*, including definitive endoderm, foregut, pancreatic endoderm, and endocrine progenitor stages (D'Amour et al., 2006; Nostro et al., 2011; Basford et al., 2012; Rezania et al., 2012). However, most protocols typically yield populations of multihormonal PSC-derived β cells (psBCs) lacking glucose responsiveness (D'Amour et al., 2006; Basford et al., 2012; Thatava et al., 2013; Cogger et al., 2017), and generation of more mature, glucose-responsive psBCs has required prolonged *in vivo* or *in vitro* maturation steps (Bruin et al., 2015a, 2015b; Kroon et al., 2008; Rezania et al., 2012).

Insulin secretion *in vivo* occurs in two distinct phases, with the first phase (0–5 min) corresponding to the release of the stored pool of insulin granules and the second phase corresponding to the release of newly formed insulin granules (Curry and MacLachlan, 1987; Pfeifer et al., 1981), and identifying the first-phase temporal insulin profile is essential for determination of proper functionality of β cells since lack of first-phase insulin-secretory response is characteristic of immature and/or dysfunctional β cells (Dhawan et al., 2015; Gerich, 2002). The dynamic perifusion system allows evaluation of temporal insulin secretion profiles in response to glucose and other secretagogs. In contrast, commonly used static glucose-stimulated insulin secretion (GSIS) assays preclude detection of the critical first-phase insulin secretion. In static GSIS assays, islets are also "bathed" with its secretory products such as insulin, amylin, and glucagon, which can affect insulin secretion and islet function and thus potentially alter the results. Another important feature of functional β cells is their responsiveness to glucagon-like peptide 1 (GLP-1), an incretin hormone regulating glucose homeostasis (Kim and Egan, 2008). Impairment of GLP-1-induced insulin secretion is frequently found in patients with T2D (Kjems et al., 2003). Recently, several groups

have demonstrated highly efficient generation of insulin-producing β cells with various key mature β-cell features from PSCs (Pagliuca et al., 2014; Rezania et al., 2014; Russ et al., 2015). However, stem cell-derived β cells did not show notable glucose and incretin responsiveness by the dynamic perifusion system or were analyzed only by static GSIS assays that do not detect the first-phase GSIS.

Studies have identified transcription factors critical for β-cell development, maturation, or function. PDX1 is expressed at the 5- to 6-somite stage and is mandatory for pancreatic organogenesis (Miki et al., 2012). PDX1 expression is followed by induction of NKX2.2 (Sussel et al., 1998) and downstream NKX6.1 (Sander et al., 2000) in pancreatic progenitor cells, which play critical roles in β-cell differentiation. In uncommitted progenitors in the developing pancreas, NEUROG3 is required for the specification of the endocrine lineage (Gradwohl et al., 2000). Specifically, transient NEUROG3 expression induces various transcription factors important for endocrine cell-lineage differentiation and β-cell function, including NEUROD1, ARX, PAX6, and ISL1 (Collombat et al., 2003). In the later stages of β-cell differentiation, MAFA and MAFB regulate β-cell formation and maturation (Artner et al., 2010). In particular, MAFA binds to a conserved insulin enhancer element RIPE3b/C1-A2 and enhances insulin gene expression as well as glucose-responsive insulin secretion (Aguayo-Mazzucato et al., 2011). In developing and mature β cells, PDX1 also binds insulin promoter to regulate insulin expression (Iype et al., 2005). Moreover, ESRRG is induced in adult β cells and plays a key role in β-cell metabolic maturation (Yoshihara et al., 2016).

Previously, we have reported inconsistent induction of PDX1 and that NKX6.1 is responsible for intrapatient variations among induced PSC (iPSC) clones in their β-cell differentiation propensities (Thatava et al., 2013). Weak in *vitro* induction of NKX6.1 also leads to lower maturation of psBCs *in vivo* (Rezania et al., 2013). We therefore hypothesized that improved β-cell specification by the introduction of key transcription factors would facilitate generation of glucose-responsive psBCs *in vitro*. In this study, we demonstrate generation of glucose- and GLP-1-responsive psBCs *in vitro* through improved β-cell specification by stepwise introduction of PDX1, NEUROG3, and MAFA (PNM) in differentiating iPSC progeny.

RESULTS

Screening of β-Cell Transcription Factor(s) for Improved Glucose- and GLP-1-Responsive Insulin Secretion in psBCs

We produced lentiviral vectors carrying codon-optimized open reading frames (ORFs) of transcription factors critical for β-cell development and function, including PDX1, NKX6.1, NKX2.2, MAFA, MAFB, NEUROD1, NEUROG3, and ESRRG (Figure 1A). Vector titers were determined by puromycin selection, and the expression of encoded transgene proteins was verified in vector-infected 293T cells by immunostaining with specific antibodies (Figure 1B). Monolayer iPSCs underwent a guided differentiation process for 3 weeks (Figure 1C). When differentiating iPSC progeny at stage 1 (S1, day 2) was transduced by a control EGFP-expressing lentiviral vector at an approximate multiplicity of infection of 30, we found EGFP signals throughout the differentiation process from S2 to S6 (Figure 1D, left panel). Flow-cytometry analysis demonstrated that over 90% of cells were EGFP positive at the end of S6 (Figure 1D, right panel). Efficient EGFP transduction was also found when iPSC progeny was transduced at other stages.

To determine whether the introduction of a single, key β-cell transcription factor could improve the glucose and GLP-1 responsiveness of psBCs, we first transduced S1 iPSC progeny with a single lentiviral vector carrying a β-cell factor. Since overexpression of PDX1, NEUROG3, and MAFA has been shown to transdifferentiate various cell types into insulin-producing cells (Zhu et al., 2017), we also transduced iPSC progeny with a combination of lentiviral vectors expressing the PNM triad at stages 1, 4, and 6, respectively. Perifusion experiments of S6 psBCs demonstrated very-low-level, non-glucose-responsive C-peptide secretion by unmodified (NULL) or EGFP vector-infected control cells (Figure 1E). Introduction of PDX1, NKX6.1, NKX2.2, MAFA, MAFB, NEUROD1, or ESRRG at S1 did not strongly affect C-peptide secretion or glucose and GLP-1 responsiveness. In contrast, introduction of NEUROG3 alone strongly enhanced the insulin-secretory capacity of resulting psBCs, from up to 0.08 pg/mL of C-peptide secretion in unmodified control psBCs and up to 36 pg/mL in NEUROG3-transduced psBCs (Figure S1). Nevertheless, NEUROG3 transduction alone did not improve glucose and GLP-1 responsiveness of resulting psBCs. Notably, stepwise transduction of PDX1, NEUROG3, and MAFA together (PNM) in differentiating iPSC progeny led within 3 weeks to the generation of psBCs with notable glucose and GLP-1 responsiveness, along with increased insulin-secretory capacity.

Stepwise PDX1, NEUROG3, and MAFA Transduction Facilitates Generation of Glucose- and GLP-1-Responsive psBCs

To assess the reproducibility of generation of glucose- and GLP-1-responsive psBCs by PNM transduction, we analyzed the dynamics of C-peptide secretion from S6 psBCs with or without PNM transduction. After confirming the expression of exogenous PDX1, NEUROG3, and MAFA

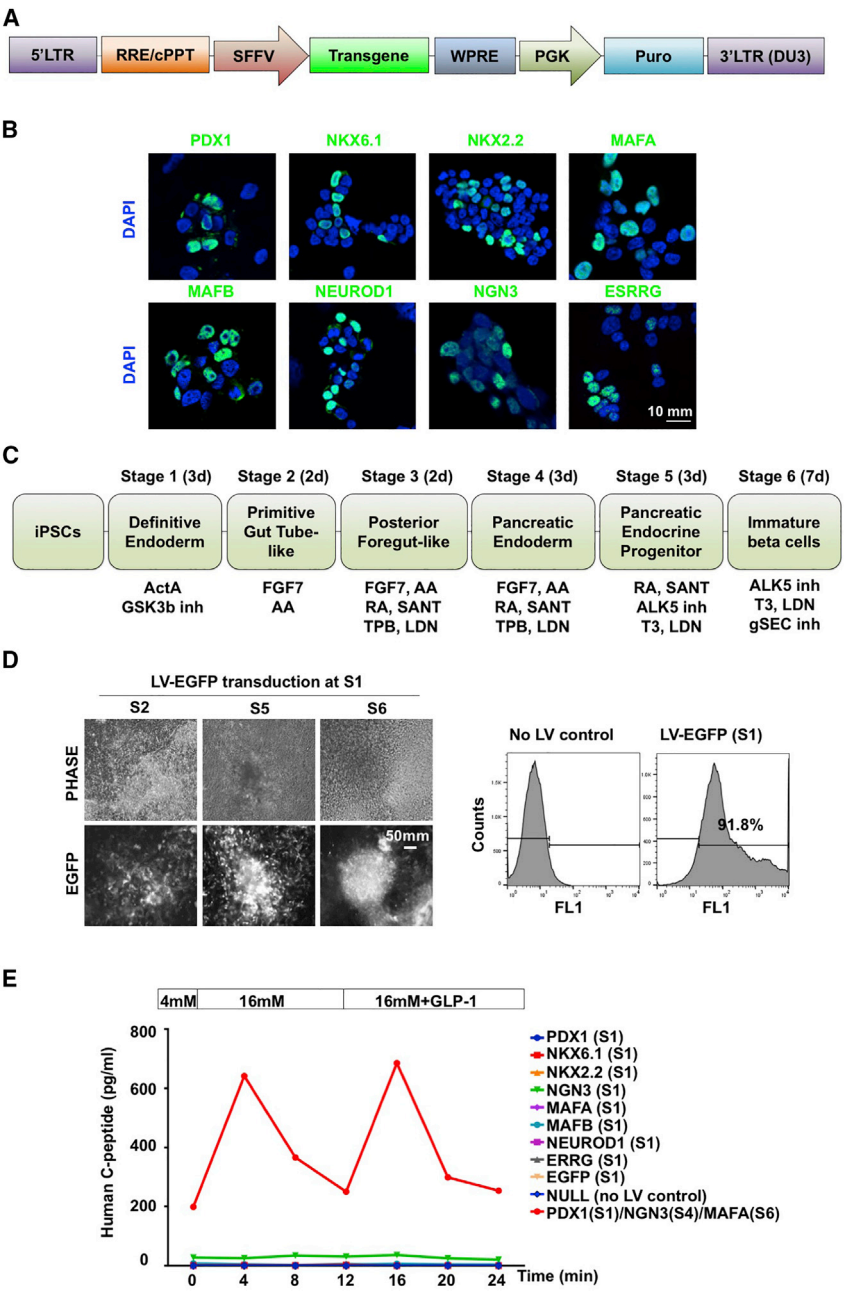

Figure 1. Screening of β-Cell Transcription Factor(s) for Improved Glucose- and GLP-1-Responsive Insulin Secretion in psBCs

(A) Schematic diagram of lentiviral vector constructs.

(B) Expression of individual β-cell factors (green). Scale bar, 10 mm.

(C) Summary of the six-stage differentiation strategy.

(D) EGFP expression monitored by UV microscope at S2, S5, and S6 (left panel). Representative fluorescence-activated cell sorting (FACS) plots for EGFP expression in control and lentiviral (LV)-EGFP transduced (S1) cells in the end of S6 stage (right panel). Phase, phase contrast. Scale bar, 50 mm.

(E) Secretion of human C peptide by psBCs in response to sequential stimulation of 4 mM, 16 mM, and 16 mM + GLP-1 glucose medium.

transgenes in S6 psBCs (Figure S2A), we observed rapid responses in C-peptide secretion from PNM-transduced S6 psBCs upon sequential increases of glucose levels from 4 to 16 mM, addition of GLP-1 to 16 mM glucose, and in 30-mM KCl depolarization (Figure 2A). The robust reaction to high glucose solution highly resembled the pattern of human islets under the same conditions (Bentsi-Barnes et al., 2011) (Figure S2B). When we assessed the fold change of C-peptide levels within individual samples at the medium-changing time points, we found a 2.1-fold increase in 16-mM glucose stimulation at the 4-min time point ($p = 0.03$), when compared with the levels at the last time point in the previous stage. We also found immediate 2.2-fold increase in 16 mM glucose + GLP-1 ($p < 0.001$), no significant change on reversion to 4 mM ($p = 0.146$), and 10.7-fold increase in KCl treatment ($p < 0.001$). Additionally, one feature of immature fetal β cells is the exaggerated insulin secretion under low glucose (Blum et al., 2012). However, we observed repressed C-peptide secretion from PNM-transduced S6 psBCs in basal 4-mM glucose

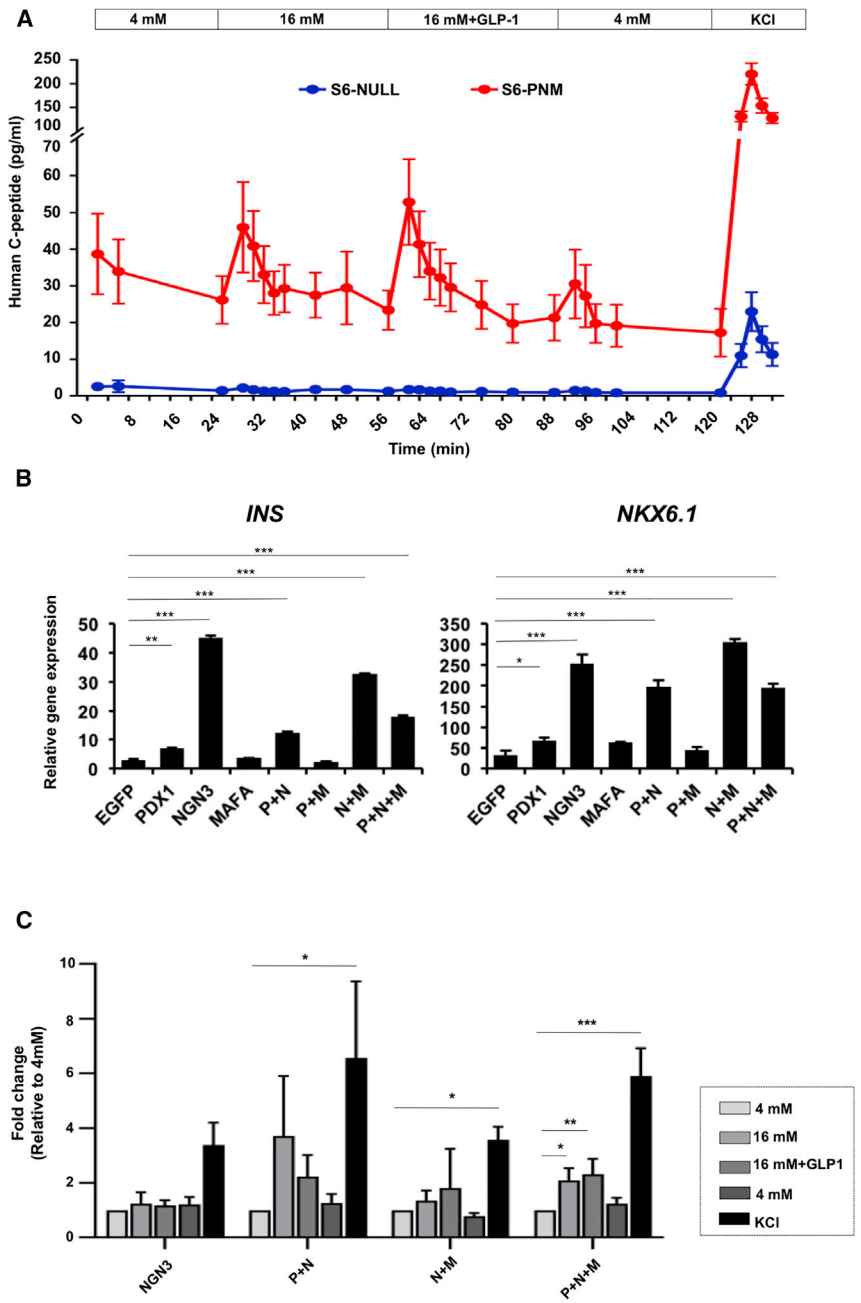

Figure 2. PNM-Transduced psBCs Are Responsive to Glucose and GLP-1 *In Vitro*

(A) Secretion of human C peptide by PNM-transduced and untransduced control psBCs (n = 3 independent experiments). Data represent the means ± SEM.

(B) Levels of *INS* and *NKX6.1* transcripts in S6 psBCs, relative to those of undifferentiated iPSCs (n = 3 independent experiments). Data represent the means ± SEM. *p < 0.05; **p < 0.01; ***p < 0.001. Student's unpaired t test.

(C) Fold changes (FC) of C-peptide levels at the 4-min time point in each stage relative to the levels at the last time point in the basal 4 mM glucose (n = 3 independent experiments). Data represent the means ± SEM. *p < 0.05; **p < 0.01; ***p < 0.001. Comparison $\log_2$ fold change, one-sample t test.

treatment. Moreover, PNM-transduced S6 psBCs also displayed a clear first- and second-phase insulin response upon 16-mM glucose treatment, which is another key feature of mature β cells (Song et al., 2000, 2002). Together, our data suggested that PNM transduction promotes the differentiation of iPSCs to glucose-responsive, incretin (GLP-1)-responsive mature β cells *in vitro*.

To further assess the contributions of PDX1 (S1), NEUROG3 (S4), and MAFA (S6), we determined the impact of transduction of different combinations of P/N/M. All psBCs that included NEUROG3 (NEUROG3 alone, PDX1 + NEUROG3, NEUROG3 + MAFA, PDX1 + NEUROG3 + MAFA) showed increased levels of *INS* and *NKX6.1* transcripts (Figure 2B). Transduction with PDX1 alone, MAFA alone, or both PDX1 and MAFA showed no significant effect (Figure 2B). When we assessed the GSIS of psBCs by the perifusion system, groups with NEUROG3 transduction exhibited higher baseline C-peptide secretion as well as higher total secretable C-peptide contents, whereas psBCs groups without NEUROG3 transduction

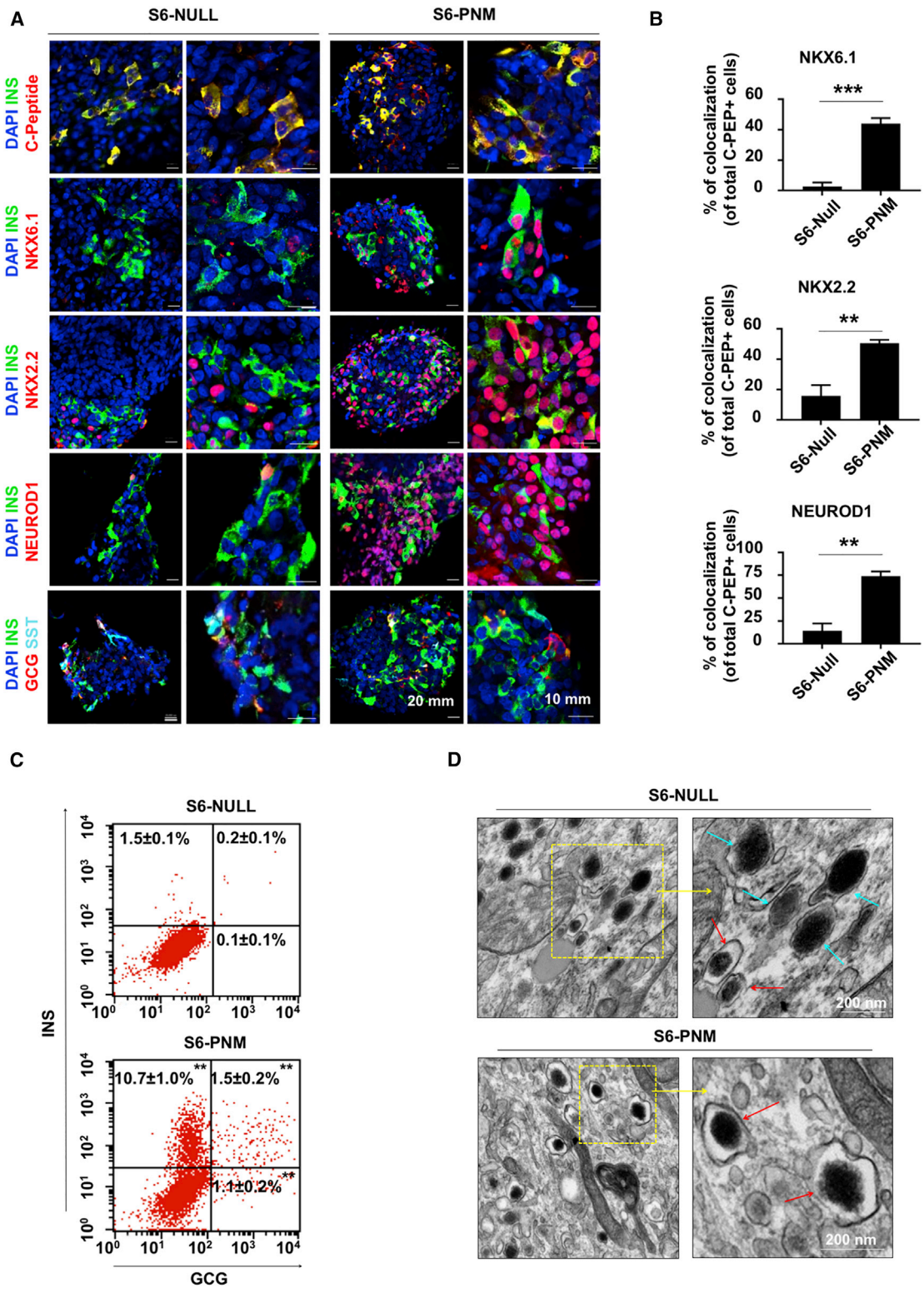

(legend on next page)

showed little C-peptide secretion (Figure S2C). Among these high C-peptide-releasing groups containing NEUROG3 transduction, only the PNM transduction group displayed significantly higher C-peptide levels at 16 mM ($p = 0.033$), 16 mM + GLP-1 ($p = 0.005$), and upon KCl depolarization ($p < 0.001$) relative to the 4-mM glucose baseline (Figure 2C). psBCs transduced with both PDX1 and NEUROG3 showed a trend of enhanced C-peptide secretion upon high glucose stimulation, whereas transduction with NEUROG3 alone or MAFA + NEUROG3 led to no significant change in glucose-responsive C-peptide secretion. These data indicate that NEUROG3 transduction is critical in generating insulin-secreting β-like cells from iPSCs, while additional PDX1 and MAFA transduction is necessary to induce glucose responsiveness in psBCs.

Mature β-Cell Characteristics Found in PNM-Transduced psBCs

We next characterized the expression of β-cell markers in PNM-transduced (S6-PNM) and control (S6-NULL) psBCs. Immunohistochemistry revealed that C-peptide signals were frequently colocalized with insulin (INS) signals in both S6-PNM and S6-NULL psBCs (Figure 3A, top row). Pancreatic α-cell marker glucagon (GCG) and δ-cell marker somatostatin (SST) signals were also found, with some multihormonal psBCs in both groups (Figure 3A, bottom row). In contrast, widespread expression of NKX6.1, NKX2.2, and NEUROD1 was only seen in S6-PNM psBCs (Figure 3A, second to fourth rows). This resulted in more frequent co-expression of NKX6.1 ($p < 0.001$), NKX2.2 ($p = 0.006$), and NEUROD1 ($p = 0.004$) in insulin-positive cells in S6-PNM compared with S6-NULL psBCs (Figure 3B). These observations indicate that stepwise PNM transduction promotes the induction of key β-cell transcription factors NKX6.1, NKX2.2, and NEUROD1 in insulin-producing cells. Flow-cytometry analysis showed that S6-PNM populations contained 12.2% insulin-positive cells, compared with 1.7% in the S6-NULL population (Figure 3C).

We also performed transmission electron microscopy analysis to characterize ultrastructures of secretory granules in S6-NULL and S6-PNM psBCs (Figure 3D). Consistent with flow-cytometry analysis, we observed more cells with endocrine granules in S6-PNM psBCs than in S6-NULL psBCs. In S6-PNM psBCs, there were numerous insulin granules with characteristic electron-dense crystal cores surrounded by a light halo, similar to normal human β-cell insulin granules (Deconinck et al., 1972). In contrast, S6-NULL psBCs often presented both insulin granules and glucagon granules characterized by larger dense cores and grayer halo (Deconinck et al., 1972). These data further support the improved maturation pattern of psBCs upon stepwise PNM transduction.

Global Gene Expression Profiling Identifies Accelerated Induction of Glucose Sensing and Insulin Secretion Genes upon PNM Transduction

To further understand the impact of PNM transduction on iPSC differentiation into psBCs, we performed next-generation RNA-sequencing analyses using RNA samples from psBCs at the end of S5 (control S5-NULL cells versus S5-PN cells, 13 days after differentiation, before S6 MAFA transduction) as well as psBCs at the end of S6 (control S6-NULL cells versus S6-PNM, 20 days after differentiation). The top 30 upregulated genes for S5-PN and S6-PNM identified key genes relevant to β-cell development and function including *INS*, *NKX2.2*, *NKX6.1*, *PAX2*, and *PCSK1* (*PC1*), as well as insulin granule exocytosis, such as *CHGA*, *SCG2/CHGC*, *SCGN*, *CPLX1*, and *CPLX2*. The major T1D antigen genes, including *INS*, *IA-2* (*PTPRN*), and *GAD65* (*GAD2*), were also prioritized. Other notable genes identified in both S5 and S6 include *SLC6A5*/*GLYT2*, which controls a glycine-insulin autocrine feedback, *BHLHE22*, regulating insulin gene expression (Melkman-Zehavi et al., 2011), and a plasma membrane Ca^{2+}-ATPase, *ATP2B2*/*PMCA2*, which affects GSIS and β-cell proliferation (Pachera et al., 2015) (Figure 4A). Further analysis of sets of genes, associated with β-cell/islet maturation, GSIS, L-type voltage-dependent calcium channel (VDCC), and ATP-sensitive potassium channel (KATP channel), also identified significant upregulation of genes underlying β-cell functionality, including *GCK*, *ESRRG*, *CHGB*, *SLC30A8*, *ABCC8*, *KCNJ11*, and *CACNA2D3* (Figure 4B). In addition, *GCG* and *SST* expression was also upregulated, especially at S5, suggesting accelerated endocrine differentiation by PDX1 and NEUROG3 transduction. qRT-PCR analysis verified upregulation of key β-cell factors in S5-PN and S6-PNM psBCs (Figure 4C). Of note, when the top 30 downregulated genes were identified for

Figure 3. Induction of NKX6.1, NKX2.2, and NEUROD1 in PNM-Transduced psBCs

(A) Representative immunofluorescent staining images of psBCs. Scale bars, 20 mm and 10 mm.

(B) Quantification of colocalization of insulin and NKX6.1, insulin and NKX2.2, or insulin and NEUROD1 in psBCs (in total n = 1,890 insulin-positive cells were counted in S6-PNM, n = 770 insulin-positive cells were counted in S6-NULL from n = 3 independent experiments). Data represent the means ± SEM. *$p < 0.05$; **$p < 0.01$; ***$p < 0.001$. Student's unpaired t test.

(C) Representative FACS plots for insulin and glucagon expression in psBCs (n = 3 independent experiments). Data represent the means ± SEM. *$p < 0.05$; **$p < 0.01$; ***$p < 0.001$. Student's unpaired t test.

(D) Representative insulin granules (red arrows) and glucagon granules (blue arrows). Scale bar, 200 nm.

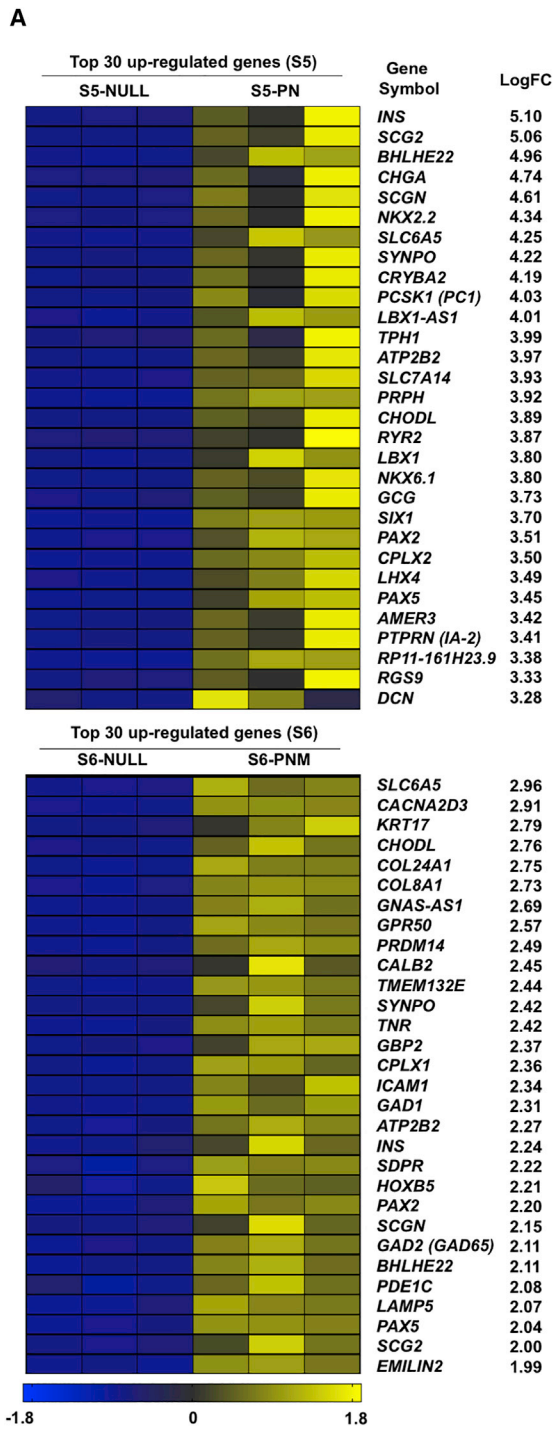

Figure 4. Global Gene Expression Profiles of PN-Transduced S5 and PNM-Transduced S6 psBCs

(A) Heatmaps of top 30 upregulated genes. LogFC stands for the $\log_2$ fold change of expression level relative to control.

(B) Summary of differentially expressed genes. LogFC stands for the $\log_2$ fold change of expression level relative to control. *$p < 0.05$. Student's unpaired t test.

(C) qRT-PCR analysis for critical β-cell genes (n = 3 independent experiments). Data represent the means ± SEM. Different letters represent statistically significant differences between two groups throughout four groups; one-way ANOVA with Tukey's test for multiple comparisons.

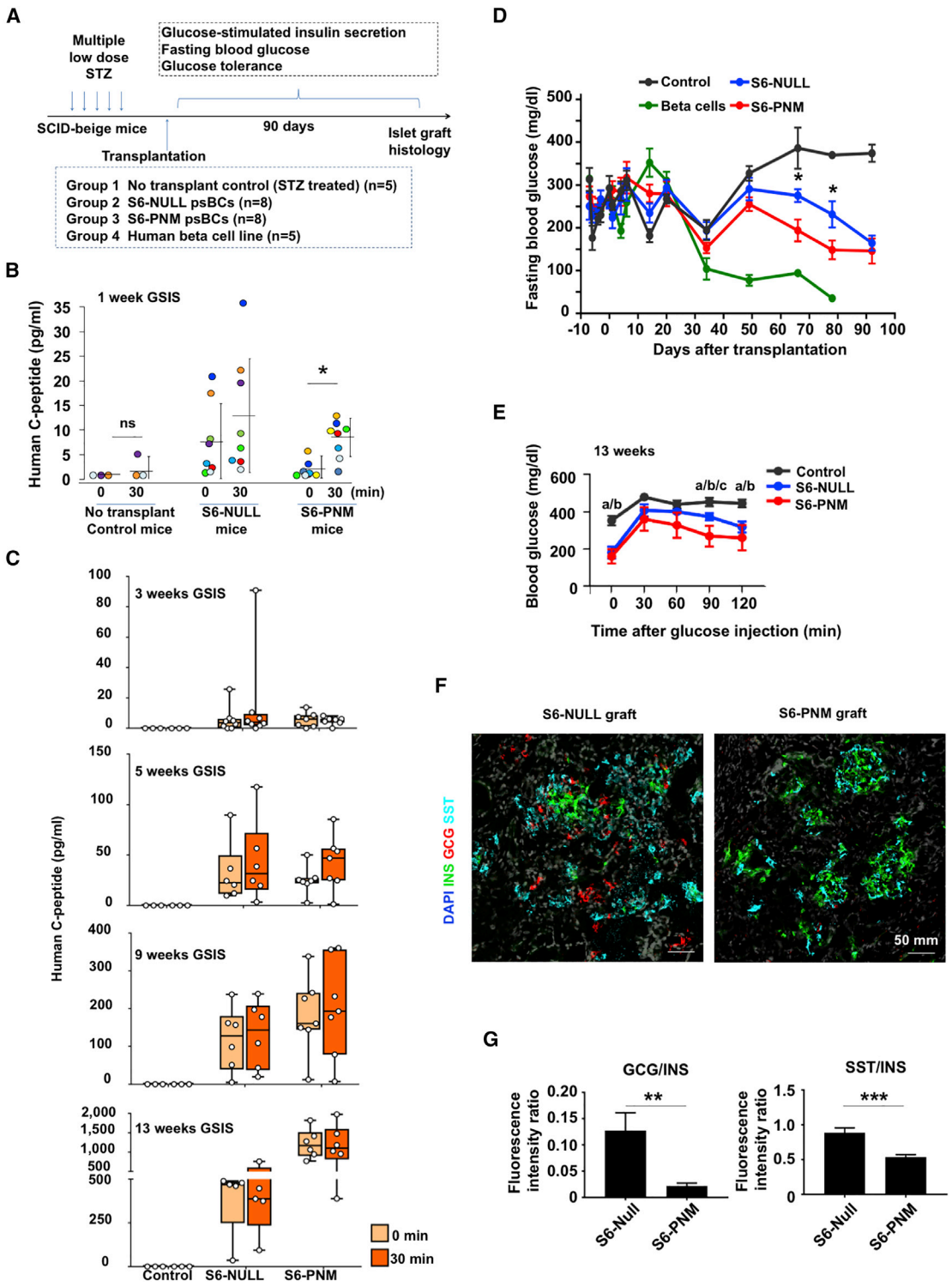

Figure 5. PNM-Transduced psBCs Show Glucose-Responsive Insulin Secretion 1 Week Post Transplantation

(A) Experimental design for *in vivo* psBC analysis.

(B and C) Fasting and 30 min (following IPGTT) human C-peptide levels in mice. C-peptide levels from individual m are shown on scale bar-and-whisker plots. Student's paired t test. ns, not significant.

(legend continued on next page)

S5-PN and S6-PNM (Figure S3A), α-fetoprotein (AFP), an extraembryonic endoderm or hepatoblast marker, was found as the most prominently suppressed gene upon PNM transduction, suggesting improved β-cell specification by PNM transduction in derived iPSC progeny. Further comparison between S5-PN and S6-PNM psBCs showed critical genes related to insulin secretion, β-cell maturation/function, and ionic channels upregulated in S6-PNM psBCs (Figures S3B and S3C). The upregulated differentially expressed genes in S6-PNM psBCs were enriched in signaling pathways including lysosome, axon guidance, insulin secretion, glutamatergic synapse, insulin signaling, endocrine, and other factor-regulated calcium reabsorption, confirming the extra benefits of MAFA transduction at S6 (Figure S3D).

PNM Transduction in Other iPSC Lines

To evaluate the robustness of PNM transduction to generate glucose- and incretin-responsive psBCs from other iPSC lines, we differentiated an additional five iPSC lines and assessed the GSIS of derived psBCs. Two iPSC lines demonstrated dynamic glucose and GLP-1 responsiveness upon PNM transduction, while three other clones showed no enhanced glucose responsiveness (Figure S4), likely due to extensive clonal variations in β-cell differentiation propensity among iPSC lines (Thatava et al., 2013).

PNM-Modified psBCs Demonstrate Glucose-Responsive Insulin Secretion *In Vivo*

To evaluate the glucose-responsive insulin-secretory capacity of PNM-modified psBCs *in vivo*, we transplanted approximately 50 million S6 psBCs into the kidney capsules of immunodeficient SCID-beige mice with streptozotocin-induced diabetes (Figure 5A). We also transplanted a human β-cell line as a control. When glucose-responsive insulin secretion was monitored upon intraperitoneal glucose administration, we found low levels of human C peptide in circulation in S6-NULL and S6-PNM recipient mice 1 week after transplantation. Importantly, levels of circulating human C peptide were significantly increased 30 min after glucose challenge in S6-PNM recipient mice ($p = 0.003$) (Figure 5B), although S6-NULL recipient mice did not show *in vivo* glucose responsiveness. No notable circulating human C peptide was seen in control mice, while mice transplanted with the human β-cell line showed no glucose responsiveness, but higher levels of human C peptide before (average 15.1 pg/mL) and after (average 18.4 pg/mL) glucose challenge. These data demonstrate the glucose-responsive insulin-secretory capacity of PNM-transduced psBCs *in vivo*, as early as 1 week post transplantation.

Fasting human C-peptide levels in S6-PNM-transplanted mice gradually increased over time, from 3 pg/mL at 1 week to 1,172 pg/mL at 13 weeks post transplantation (Figure S5A). GSIS was not detected at 3, 5, 9, and 13 weeks (Figure 5C). Similar results were found in S6-NULL-transplanted mice (Figure 5C). However, fasting circulating C-peptide levels were significantly lower in S6-NULL than those observed in S6-PNM at weeks 11 ($p = 0.047$) and 13 ($p = 0.048$) (Figure S5A). Similarly, although blood glucose levels after 16 h of fasting remained high in both S6-NULL and S6-PNM psBCs-transplanted mice for 3 weeks, S6-NULL- and S6-PNM-recipient mice started to show lower blood glucose levels than controls at 8 weeks post transplant (Figure 5D). The blood glucose levels were significantly lower in S6-PNM mice than those in S6-NULL mice at 9 ($p = 0.022$) and 11 ($p = 0.047$) weeks post transplant (Figure 5D). To assess the impact of psBC transplantation on the glucose tolerance *in vivo*, we also conducted an intraperitoneal glucose tolerance test (IPGTT) at 7 and 13 weeks post transplant. There was no difference observed in glucose levels among diabetic controls, S6-NULL recipient, and S6-PNM recipient mice at 7 weeks (Figure S5B). However, at 13 weeks, S6-PNM recipient mice displayed lower glucose levels than S6-NULL at 90 min ($p = 0.003$), indicating superior glucose regulation by S6-PNM over S6-NULL psBCs (Figure 5E).

Prospectively, 13 weeks after transplantation, we harvested the kidneys with psBC grafts from the recipient mice. Further analysis revealed that the insulin-positive cells in S6-PNM and S6-NULL grafts were largely monohormonal. However, S6-PNM grafts contained rich clusters of insulin-positive cells, whereas in S6-NULL grafts the insulin-positive cells were scattered (Figure 5F). Notably, insulin-positive cells in S6-NULL were accompanied by significantly more glucagon-positive ($p = 0.007$) and somatostatin-positive cells ($p < 0.001$) compared with S6-PNM (Figure 5G),

(D) Fasting blood glucose levels after transplantation in mice. Data represent the means ± SEM. Comparison of S6-PNM with S6-NULL, *$p < 0.05$. Student's unpaired t test.

(E) Blood glucose levels during IPGTT in mice. Data represent the means ± SEM. "a" represents a statistically significant difference between control and S6-PNM, "b" represents a difference between control and S6-NULL, "c" represents a difference between S6-NULL and S6-PNM; one-way ANOVA with Tukey's test for multiple comparisons.

(F) Representative immunofluorescent staining images of psBC grafts. Scale bar, 50 mm.

(G) Fluorescence intensity ratios of GCG to INS and SST to INS in images of S6-NULL ($n = 22$ images, 5–6 images per mouse, 4 mice were analyzed) and S6-PNM ($n = 23$ images, 5–6 images per mouse, 4 mice were analyzed) grafts. Data represent the means ± SEM. *$p < 0.05$; **$p < 0.01$; ***$p < 0.001$. Student's unpaired t test.

suggesting that the less mature S6-NULL cells may further adopt α-cell and δ-cell destiny *in vivo*.

DISCUSSION

Despite extensive progress in human PSC differentiation protocols, *in vitro* generation of functional psBCs with dynamic glucose and incretin responsiveness has been an ongoing challenge limiting the derivation of competent cell therapies (Holditch et al., 2014). Most protocols failed to show the first-phase insulin secretion of their β-cell products upon glucose and GLP-1 stimulations. Additionally, GSIS of psBCs has been assessed mainly by static GSIS assays, which do not monitor first-phase GSIS and can be affected by varying metabolites secreted by the cells during the long incubation period with glucose. Here we assessed psBCs in a perifusion system that mimics the physiological glycemic environment and detects the first-phase GSIS. Our data demonstrated that stepwise introduction of key transcription factors PDX1, NEUROG3, and MAFA achieved reproducible generation of glucose- and GLP-1-responsive psBCs *in vitro*. PNM transduction accelerated psBC maturation through enhanced induction of key β-cell factors related to glucose sensing and insulin secretion. PNM transduction also improved β-cell specification, implicated by potent induction of important β-cell factors, such as NEUROD1, NKX6.1, NKX2.2, GCK, and GLP1R, while suppressing the extraembryonic endoderm or hepatoblast marker AFP. Our study therefore suggests PNM transduction facilitates *in vitro* generation of functional β cells from human PSCs through improved β-cell specification. The pre-achieved organotypic phenotype offered a proficient biotherapeutics capable to reverse symptoms of diabetes post transplantation.

Neonatal β cells are characterized by poor glucose responsiveness with a generalized immaturity of the metabolic pathways, and only gain robust glucose responsiveness several weeks after birth (Jermendy et al., 2011). Human psBCs typically show characteristics reminiscent of neonatal β cells. Various studies have demonstrated generation of glucose-responsive psBCs through *in vivo* maturation (Kroon et al., 2008; Rezania et al., 2014), with more accelerated maturation in rats than mice (Bruin et al., 2015a, 2015b). Those observations indicate the roles of extracellular stimuli for acquisition of mature β-cell fate. Accordingly, the field has been searching for small molecules/growth factors that can induce maturation of psBCs, and identified factors, such as thyroid hormone or β-cellulin, that have been included in prolonged *in vitro* psBC maturation processes (Aguayo-Mazzucato et al., 2013; Pagliuca et al., 2014; Rezania et al., 2014; Russ et al., 2015). We showed that PNM transduction facilitates generation of glucose- and GLP-1-responsive psBCs in 3 weeks without prolonged *in vitro* culture or *in vivo* additional maturation steps, implying that PNM transduction can substitute critical external stimuli provided through *in vivo* maturation or prolonged *in vitro* maturation steps. Considering that NEUROG3 alone can strongly enhance expression of INS and NKX6.1 and insulin-secretory capacity, this further supports that NEUROG3 transduction plays the key role in improved iPSC differentiation into mature β cells upon PNM transduction (McGrath et al., 2015) Additionally, transduction of MAFA, the major transcription factor for β-cell maturation in neonatal β cells, contributes to the accelerated psBC maturation. However, single MAFA transduction at S1 or transduction of S4 NEUROG3 plus S5 MAFA failed to induce glucose responsiveness in psBCs, indicating that MAFA and NEUROG3 transduction are not sufficient for reproducible *in vitro* psBC maturation. In contrast, psBCs with dual PDX1 and NEUROG3 transduction showed a trend of GSIS, suggesting an important role of PDX1 transduction in accelerated psBC maturation. Since PDX1 deficiency impairs GSIS through mitochondrial dysfunction (Gauthier et al., 2009), it is plausible that PDX1 transduction contributes to GSIS in psBCs in addition to improved pancreatic specification. Use of an inducible transgene expression system for PNM transduction/shutdown will clarify the contributions of each factor to improved iPSC differentiation or psBC maturation.

Previous studies have demonstrated that simultaneous transduction of PDX1, NEUROG3, and MAFA achieves transdifferentiation of pancreatic exocrine, liver, or intestine cells into insulin-producing cells (Zhu et al., 2017). However, these (re)differentiation strategies appeared to be insufficient in generating authentic β cells that display β-cell morphology and robust glucose and incretin responsiveness. Recently, Saxena et al. (2016) reported improved psBC generation from iPSCs through the introduction of two expression constructs; one for bicistronic PDX1-MAFA fusion protein linked by a self-cleaving 2A peptide and another for NEUROG3. Derived psBCs showed glucose responsiveness by a static GSIS assay. In contrast to prior studies, our study delivered PNM at different steps during iPSCs-to-β-cell differentiating process based on known expressing patterns of each factor (Brissova et al., 2002; Gradwohl et al., 2000; Holland et al., 2002; Matsuoka et al., 2003, 2004). Specifically, we delivered PNM at stages 1, 4, and 6, respectively. Our stepwise gene delivery strategy strongly enhanced iPSC differentiation into mature β cells, resulting in generation of functional psBCs with clear glucose and GLP-1 responsiveness, demonstrated by a real-time GSIS assay underscoring the permissive timeline of sequential tissue-specific programming.

Insulin is secreted through granule exocytosis. In response to glucose metabolism, inhibition of KATP

channels and elevation of intracellular calcium levels lead to insulin vesicle fusion to the β-cell membrane with insulin secretion disorders precipitated by KATP channelopathy (Gauthier and Wollheim, 2008; Olson and Terzic, 2010; Takahashi et al., 2010). Intriguingly, PNM modification led to upregulation of genes involved in insulin release and VDCC- and KATP-channel activities, such as *ABCC8* (Babenko et al., 2006), *KCNJ11* (Gloyn et al., 2004), *CACNA1D* (Reinbothe et al., 2013), and *SCGN* (Yang et al., 2016). Other genes critical in glucose sensing or insulin secretion were also largely elevated, including *SLC6A5* (Yan-Do et al., 2016), *ESRRG* (Yoshihara et al., 2016), *SLC30A8* (Wijesekara et al., 2010), and *GCK* (Matschinsky et al., 2006). Intriguingly, *SLC6A5* was identified as one of the top upregulated genes upon PNM transduction. *SLC6A5* regulates the expression of glycine transporter 2 (*GlyT2*), which is expressed on human β cells and mediates the transportation of glycine, a neurotransmitter critical for coordinating insulin secretion by modulating the electrical activity of β cells via ionic channels and receptors. Additionally, PNM transduction enhanced *GLP1R* expression, which likely sensitized derived psBCs to incretin stimulation. These observations highlight the multifaceted effects of PNM transduction during iPSC differentiation into functional psBCs. Comparing our protocol with previously reported protocols is warranted in order to further understand the mechanism and inform future studies.

Previously, we have reported prominent intrapatient variations in psBC differentiation propensities among iPSC clones from T1D patients (Thatava et al., 2013). We found that PNM transduction led to more consistent generation of mature psBCs from iPSCs. Since PNM transduction strongly enhanced expression of major T1D antigen genes, such as *INS*/*Proinsulin*, *PTPRN*/*IA-2*, and *GAD2*/*GAD65*, PNM-modified psBCs from T1D patients would provide excellent research tools to model patient-specific autoimmune responses to β cells *in vitro*.

We also found that single transduction of PDX1, MAFA, NEUROD1, NKX2.2, NKX6.1, MAFB, or ESRRG alone did not improve insulin secretion or glucose responsiveness of psBCs. This is likely due to insufficient β-cell specification in the absence of trans-supplementation of NEUROG3. It is noteworthy that endogenous *NEUROD1*, *NKX2.2*, *NKX6.1*, and *ESRRG* were all highly upregulated upon PNM transduction, suggesting limited additive β-cell maturation effects by additional NEUROD1, NKX2.2, NKX6.1, and ESRRG transduction in PNM-modified psBCs.

We acknowledge that a yield of 12% insulin-positive cells upon PNM transduction is relatively low when compared with previous studies mainly using embryonic stem cells (Kroon et al., 2008; Pagliuca et al., 2014; Rezania et al., 2014). This is largely due to the high clonal and intrapatient variations in iPSC differentiation into insulin-producing cells, as we and others have described (Tateishi et al., 2008; Maehr et al., 2009; Thatava et al., 2013). It is also notable that introduction of NEUROG3 alone strongly enhanced induction of insulin gene; however, derived cells failed to show glucose responsiveness (Figures 2B and 2C). Very recently we found a small molecule that strongly enhanced iPSC differentiation into insulin-positive β cells (J.M.T. et al., unpublished data [manuscript in preparation]). With this small molecule, we were able to make up to 20% insulin-positive cells from iPSC clone BM9 without PNM introduction. However, these cells did not show glucose responsiveness by the perifusion system. These observations suggest that generation of insulin-producing cells and induction of glucose responsiveness in insulin-positive cells are regulated by independent mechanisms. With our stepwise PNM transduction strategy, we clearly demonstrated that PNM addition improved the differentiation efficiency and, more importantly, improved the quality of derived β cells, which marks considerable progress compared with previous studies. It is also noteworthy that our data provide an important implication for future translational applications. Improved PNM expression by clinically relevant strategies, such as RNA transfection or addition of small molecules or cytokines to enhance expression of endogenous PNM factors, together with PSC lines with high β-cell differentiation propensity, would allow more mature β-cell generation from PSCs for transplantation.

After transplanting the PNM-transduced psBCs into immunodeficient diabetic mice, we were able to detect glucose-responsive human C-peptide secretion as early as 1 week after surgery, indicating the functionality of psBCs *in vivo*. However, the levels of C-peptide secretion were low and we found no effects on glucose handling or fasting blood glucose levels until 9 weeks post transplantation, possibly due to slower vascularization (Mattsson et al., 2002) and adaptation of the transplanted cells. Nevertheless, PNM-transduced cells exhibited better diabetes-reversal effects, better glucose-clearance ability, and richer expression of insulin in excised grafts, indicating a therapeutic effect superior to that of S6-NULL psBCs. Unexpectedly, we did not see obvious GSIS by 30-min IPGTT tests in S6-PNM psBCs. We speculate that sustained NEUROG3 expression in PNM-transduced psBCs had negative impacts on long-term psBC function. Further analysis using an inducible NEUROG3-expression vector will elucidate the influence of NEUROG3 expression on sustained psBC functionality *in vivo*.

In summary, our study demonstrates successful generation of glucose- and GLP-1-responsive psBCs *in vitro* using a streamlined multifactor approach to ensure pre-emptive differentiation and lasting organotypic orientation after

transplantation. While lineage-specification protocols have been implemented in regenerative clinical development strategies within and beyond (Terzic and Behfar, 2016) endocrinology, adoption of a reproducible and scalable platform for derivation of competent and proficient biologics would further accelerate diagnostic and therapeutic applications.

EXPERIMENTAL PROCEDURES

Cells

Commercially available iPSC lines IISH2i-BM9 (WiCell, Madison, WI), and in-house iPSC lines #A, #B, #C, #D, and #E were tested for β-cell propensity.

Lentiviral Vectors

Lentiviral vector genome plasmid, pSIN-CSGW-PKG-puro, which supports EGFP expression and puromycin selection, was kindly provided by Dr. Paul Lehner (Cambridge Institute for Medical Research). Codon-optimized ORF sequences for β-cell factors, including PDX1, NEUROG3, NKX2.2, NKX6.1, NEUROD1, MAFA, MAFB, and ESRRG, were designed and synthesized (GenScript, Piscataway, NJ), and cloned into the place of the EGFP gene in pSIN-CSGW-PKG-puro with the unique *Bam*HI and *Xho*I sites.

Guided Differentiation and Stepwise Lentiviral Vector Transduction

The basic differentiation strategy without viral vector transduction was a modified version of the previously published protocols. The detailed differentiation protocol is available in Supplemental Information.

qRT-PCR

For qRT-PCR, total RNA from differentiated iPSCs at indicated time points was isolated using TRIzol according to the manufacturer's instructions. cDNAs were then synthesized by reverse transcription from 200 ng of total RNA. The sequences of the primers used for qRT-PCR are listed in Table S1.

RNA Sequencing

For RNA sequencing, a total of 200 ng of RNA from differentiated iPSCs at indicated time points was isolated using an RNeasy Mini Kit. Library preparation (TruSeq mRNA v2 [TMRNA]) and next-generation sequencing and analysis (standard secondary analysis pipeline, MAPRSeq) were performed in the Mayo Clinic Sequencing and Bioinformatics Cores. GEO: GSE133731.

Immunofluorescence Staining

Lentiviral vector-infected 293T cells, undifferentiated iPSCs, and cryosections of mouse kidneys with the grafts were fixed with 4% paraformaldehyde (PFA) for 20 min. After fixation, cells were washed once with PBS and permeabilized with 0.3% Triton X-100 in PBS for 10 min. Cells were then washed with PBS twice and blocked with 5% fetal bovine serum (FBS) in PBS for 1 h. Cells were incubated overnight with specific antibodies at 4°C, followed by incubation with secondary antibodies for 1 h at room temperature.

Flow Cytometry

iPSC-derived psBCs were dispersed into single-cell suspension. Cells were incubated overnight with specific antibodies at 4°C. After washing three times with 5% FBS, cells were stained with secondary antibodies. Cells were then washed and filtered through a 35-μm mesh Falcon tube, and analyzed using the LSR-II flow cytometer (BD Biosciences). Analysis of the results was performed using FlowJo software.

Electron Microscopy

iPSC-derived psBCs were fixed at room temperature. Cell samples were processed and analyzed by transmission electron microscopy at the Mayo Clinic Microscopy and Cell Analysis Core.

In Vitro GSIS Assay

We used an islet perifusion system (Biorep Technologies, Miami Lakes, FL). Detailed methods are available in Supplemental Information.

Mice Transplantation Studies

All animal experiments were performed in accordance with Mayo Clinic International Animal Care and Use Committee regulations. Immunodeficient Fox Chase SCID-Beige mice, aged 8–10 weeks, were purchased from Charles River Laboratory. Detailed methods are available in Supplemental Information.

Intraperitoneal Glucose Tolerance Test

For measurement of glucose-handling capacity *in vivo*, mice were fasted (16 h) and blood glucose was tested at 0, 30, 60, 90, and 120 min after intraperitoneal injection of D-(+)-glucose at 2 g/kg body weight.

Sample Size and Statistical Analysis

All data represent the means ± SEM of three to nine samples, as indicated in the figure legends. Group comparisons were analyzed by unpaired or paired t tests, one-sample t test, and one-way ANOVA with Tukey's test using IBM SPSS Statistics v.22. Bar graphs, heatmaps, curves, and box-and-whisker plots were generated with GraphPad Prism7 and Excel 2010. Detailed methods are available in Supplemental Information.

Data Availability

All relevant data are available from the corresponding author on request.

SUPPLEMENTAL INFORMATION

Supplemental Information can be found online at https://doi.org/10.1016/j.stemcr.2019.07.006.

AUTHOR CONTRIBUTIONS

Y.Z. carried out all the experiments, analyzed the data, and prepared the manuscript. J.M.T. contributed to lentiviral production,

animal experiments, and results interpretation. C.A.S. provided help in cell culture and data analysis. Q.L. provided advice on the manuscript and contributed to figure preparation. Z.Z. commented on the manuscript. K.R. and A.V.M. assisted with the perifusion experiments and provided generous advice on results interpretation. A.T., D.W., and Y.C.K. discussed the results and commented on the manuscript. Y.I. supervised the project, oversaw the preparation of the manuscript, commented on and revised the manuscript, and provided funding for all related work. All authors read and approved the final manuscript.

ACKNOWLEDGMENTS

The authors would like to thank Brian Lu and Salma Morsy for their advice on experimental techniques. This work is supported by Sheikh Khalifa Bin Zayed Al Nahyen Regenerative Diabetes Research Program, Mayo Center for Regenerative Medicine, Regenerative Medicine Minnesota, Vann Family Fund in Diabetes Research, Kendrick Foundation, Paul A. and Ruth M. Schilling Medical Research Endowment Fund, and NIH 1R43GM112316-01A.

Received: June 27, 2018
Revised: July 6, 2019
Accepted: July 8, 2019
Published: August 1, 2019

REFERENCES

Aguayo-Mazzucato, C., Koh, A., El Khattabi, I., Li, W.C., Toschi, E., Jermendy, A., Juhl, K., Mao, K., Weir, G.C., Sharma, A., et al. (2011). Mafa expression enhances glucose-responsive insulin secretion in neonatal rat beta cells. Diabetologia *54*, 583–593.

Aguayo-Mazzucato, C., Zavacki, A.M., Marinelarena, A., Hollister-Lock, J., El Khattabi, I., Marsili, A., Weir, G.C., Sharma, A., Larsen, P.R., and Bonner-Weir, S. (2013). Thyroid hormone promotes postnatal rat pancreatic beta-cell development and glucose-responsive insulin secretion through MAFA. Diabetes *62*, 1569–1580.

Artner, I., Hang, Y., Mazur, M., Yamamoto, T., Guo, M., Lindner, J., Magnuson, M.A., and Stein, R. (2010). MafA and MafB regulate genes critical to beta-cells in a unique temporal manner. Diabetes *59*, 2530–2539.

Babenko, A.P., Polak, M., Cave, H., Busiah, K., Czernichow, P., Scharfmann, R., Bryan, J., Aguilar-Bryan, L., Vaxillaire, M., and Froguel, P. (2006). Activating mutations in the ABCC8 gene in neonatal diabetes mellitus. N. Engl. J. Med. *355*, 456–466.

Basford, C.L., Prentice, K.J., Hardy, A.B., Sarangi, F., Micallef, S.J., Li, X., Guo, Q., Elefanty, A.G., Stanley, E.G., Keller, G., et al. (2012). The functional and molecular characterisation of human embryonic stem cell-derived insulin-positive cells compared with adult pancreatic beta cells. Diabetologia *55*, 358–371.

Bentsi-Barnes, K., Doyle, M.E., Abad, D., Kandeel, F., and Al-Abdullah, I. (2011). Detailed protocol for evaluation of dynamic perifusion of human islets to assess beta-cell function. Islets *3*, 284–290.

Blum, B., Hrvatin, S.S., Schuetz, C., Bonal, C., Rezania, A., and Melton, D.A. (2012). Functional beta-cell maturation is marked by an increased glucose threshold and by expression of urocortin 3. Nat. Biotechnol. *30*, 261–264.

Brissova, M., Shiota, M., Nicholson, W.E., Gannon, M., Knobel, S.M., Piston, D.W., Wright, C.V., and Powers, A.C. (2002). Reduction in pancreatic transcription factor PDX-1 impairs glucose-stimulated insulin secretion. J. Biol. Chem. *277*, 11225–11232.

Bruin, J.E., Asadi, A., Fox, J.K., Erener, S., Rezania, A., and Kieffer, T.J. (2015a). Accelerated maturation of human stem cell-derived pancreatic progenitor cells into insulin-secreting cells in immunodeficient rats relative to mice. Stem Cell Reports *5*, 1081–1096.

Bruin, J.E., Saber, N., Braun, N., Fox, J.K., Mojibian, M., Asadi, A., Drohan, C., O'Dwyer, S., Rosman-Balzer, D.S., Swiss, V.A., et al. (2015b). Treating diet-induced diabetes and obesity with human embryonic stem cell-derived pancreatic progenitor cells and antidiabetic drugs. Stem Cell Reports *4*, 605–620.

Butler, A.E., Janson, J., Bonner-Weir, S., Ritzel, R., Rizza, R.A., and Butler, P.C. (2003). Beta-cell deficit and increased beta-cell apoptosis in humans with type 2 diabetes. Diabetes *52*, 102–110.

Cogger, K.F., Sinha, A., Sarangi, F., McGaugh, E.C., Saunders, D., Dorrell, C., Mejia-Guerrero, S., Aghazadeh, Y., Rourke, J.L., Screaton, R.A., et al. (2017). Glycoprotein 2 is a specific cell surface marker of human pancreatic progenitors. Nat. Commun. *8*, 331.

Collombat, P., Mansouri, A., Hecksher-Sorensen, J., Serup, P., Krull, J., Gradwohl, G., and Gruss, P. (2003). Opposing actions of Arx and Pax4 in endocrine pancreas development. Genes Dev. *17*, 2591–2603.

Curry, D.L., and MacLachlan, S.A. (1987). Synthesis-secretion coupling of insulin: effect of aging. Endocrinology *121*, 241–247.

D'Amour, K.A., Bang, A.G., Eliazer, S., Kelly, O.G., Agulnick, A.D., Smart, N.G., Moorman, M.A., Kroon, E., Carpenter, M.K., and Baetge, E.E. (2006). Production of pancreatic hormone-expressing endocrine cells from human embryonic stem cells. Nat. Biotechnol. *24*, 1392–1401.

Deconinck, J.F., Van Assche, F.A., Potvliege, P.R., and Gepts, W. (1972). The ultrastructure of the human pancreatic islets. II. The islets of neonates. Diabetologia *8*, 326–333.

Dhawan, S., Tschen, S.I., Zeng, C., Guo, T., Hebrok, M., Matveyenko, A., and Bhushan, A. (2015). DNA methylation directs functional maturation of pancreatic beta cells. J. Clin. Invest. *125*, 2851–2860.

Gauthier, B.R., Wiederkehr, A., Baquie, M., Dai, C., Powers, A.C., Kerr-Conte, J., Pattou, F., MacDonald, R.J., Ferrer, J., and Wollheim, C.B. (2009). PDX1 deficiency causes mitochondrial dysfunction and defective insulin secretion through TFAM suppression. Cell Metab. *10*, 110–118.

Gauthier, B.R., and Wollheim, C.B. (2008). Synaptotagmins bind calcium to release insulin. Am. J. Physiol. Endocrinol. Metab. *295*, E1279–E1286.

Gerich, J.E. (2002). Is reduced first-phase insulin release the earliest detectable abnormality in individuals destined to develop type 2 diabetes? Diabetes *51* (*Suppl 1*), S117–S121.

Gloyn, A.L., Pearson, E.R., Antcliff, J.F., Proks, P., Bruining, G.J., Slingerland, A.S., Howard, N., Srinivasan, S., Silva, J.M., Molnes, J., et al. (2004). Activating mutations in the gene encoding the

ATP-sensitive potassium-channel subunit Kir6.2 and permanent neonatal diabetes. N. Engl. J. Med. *350*, 1838–1849.

Gradwohl, G., Dierich, A., LeMeur, M., and Guillemot, F. (2000). neurogenin3 is required for the development of the four endocrine cell lineages of the pancreas. Proc. Natl. Acad. Sci. U S A *97*, 1607–1611.

Holditch, S.J., Terzic, A., and Ikeda, Y. (2014). Concise review: pluripotent stem cell-based regenerative applications for failing beta-cell function. Stem Cells Transl. Med. *3*, 653–661.

Holland, A.M., Hale, M.A., Kagami, H., Hammer, R.E., and MacDonald, R.J. (2002). Experimental control of pancreatic development and maintenance. Proc. Natl. Acad. Sci. U S A *99*, 12236–12241.

Iype, T., Francis, J., Garmey, J.C., Schisler, J.C., Nesher, R., Weir, G.C., Becker, T.C., Newgard, C.B., Griffen, S.C., and Mirmira, R.G. (2005). Mechanism of insulin gene regulation by the pancreatic transcription factor Pdx-1: application of pre-mRNA analysis and chromatin immunoprecipitation to assess formation of functional transcriptional complexes. J. Biol. Chem. *280*, 16798–16807.

Jermendy, A., Toschi, E., Aye, T., Koh, A., Aguayo-Mazzucato, C., Sharma, A., Weir, G.C., Sgroi, D., and Bonner-Weir, S. (2011). Rat neonatal beta cells lack the specialised metabolic phenotype of mature beta cells. Diabetologia *54*, 594–604.

Kim, W., and Egan, J.M. (2008). The role of incretins in glucose homeostasis and diabetes treatment. Pharmacol. Rev. *60*, 470–512.

Kjems, L.L., Holst, J.J., Volund, A., and Madsbad, S. (2003). The influence of GLP-1 on glucose-stimulated insulin secretion: effects on beta-cell sensitivity in type 2 and nondiabetic subjects. Diabetes *52*, 380–386.

Kroon, E., Martinson, L.A., Kadoya, K., Bang, A.G., Kelly, O.G., Eliazer, S., Young, H., Richardson, M., Smart, N.G., Cunningham, J., et al. (2008). Pancreatic endoderm derived from human embryonic stem cells generates glucose-responsive insulin-secreting cells in vivo. Nat. Biotechnol. *26*, 443–452.

Maehr, R., Chen, S., Snitow, M., Ludwig, T., Yagasaki, L., Goland, R., Leibel, R.L., and Melton, D.A. (2009). Generation of pluripotent stem cells from patients with type 1 diabetes. Proc. Natl. Acad. Sci. U S A *106*, 15768–15773.

Matschinsky, F.M., Magnuson, M.A., Zelent, D., Jetton, T.L., Doliba, N., Han, Y., Taub, R., and Grimsby, J. (2006). The network of glucokinase-expressing cells in glucose homeostasis and the potential of glucokinase activators for diabetes therapy. Diabetes *55*, 1–12.

Matsuoka, T.A., Artner, I., Henderson, E., Means, A., Sander, M., and Stein, R. (2004). The MafA transcription factor appears to be responsible for tissue-specific expression of insulin. Proc. Natl. Acad. Sci. U S A *101*, 2930–2933.

Matsuoka, T.A., Zhao, L., Artner, I., Jarrett, H.W., Friedman, D., Means, A., and Stein, R. (2003). Members of the large Maf transcription family regulate insulin gene transcription in islet beta cells. Mol. Cell. Biol. *23*, 6049–6062.

Mattsson, G., Jansson, L., and Carlsson, P.O. (2002). Decreased vascular density in mouse pancreatic islets after transplantation. Diabetes *51*, 1362–1366.

McGrath, P.S., Watson, C.L., Ingram, C., Helmrath, M.A., and Wells, J.M. (2015). The basic helix-loop-helix transcription factor NEUROG3 is required for development of the human endocrine pancreas. Diabetes *64*, 2497–2505.

Melkman-Zehavi, T., Oren, R., Kredo-Russo, S., Shapira, T., Mandelbaum, A.D., Rivkin, N., Nir, T., Lennox, K.A., Behlke, M.A., Dor, Y., et al. (2011). miRNAs control insulin content in pancreatic beta-cells via downregulation of transcriptional repressors. EMBO J. *30*, 835–845.

Miki, R., Yoshida, T., Murata, K., Oki, S., Kume, K., and Kume, S. (2012). Fate maps of ventral and dorsal pancreatic progenitor cells in early somite stage mouse embryos. Mech. Dev. *128*, 597–609.

Nostro, M.C., Sarangi, F., Ogawa, S., Holtzinger, A., Corneo, B., Li, X., Micallef, S.J., Park, I.H., Basford, C., Wheeler, M.B., et al. (2011). Stage-specific signaling through TGFbeta family members and WNT regulates patterning and pancreatic specification of human pluripotent stem cells. Development *138*, 861–871.

Ogurtsova, K., da Rocha Fernandes, J.D., Huang, Y., Linnenkamp, U., Guariguata, L., Cho, N.H., Cavan, D., Shaw, J.E., and Makaroff, L.E. (2017). IDF Diabetes Atlas: global estimates for the prevalence of diabetes for 2015 and 2040. Diabetes Res. Clin. Pract. *128*, 40–50.

Olson, T.M., and Terzic, A. (2010). Human K(ATP) channelopathies: diseases of metabolic homeostasis. Pflugers Arch. *460*, 295–306.

Pachera, N., Papin, J., Zummo, F.P., Rahier, J., Mast, J., Meyerovich, K., Cardozo, A.K., and Herchuelz, A. (2015). Heterozygous inactivation of plasma membrane Ca(2+)-ATPase in mice increases glucose-induced insulin release and beta cell proliferation, mass and viability. Diabetologia *58*, 2843–2850.

Pagliuca, F.W., Millman, J.R., Gurtler, M., Segel, M., Van Dervort, A., Ryu, J.H., Peterson, Q.P., Greiner, D., and Melton, D.A. (2014). Generation of functional human pancreatic beta cells in vitro. Cell *159*, 428–439.

Pfeifer, M.A., Halter, J.B., and Porte, D., Jr. (1981). Insulin secretion in diabetes mellitus. Am. J. Med. *70*, 579–588.

Reinbothe, T.M., Alkayyali, S., Ahlqvist, E., Tuomi, T., Isomaa, B., Lyssenko, V., and Renstrom, E. (2013). The human L-type calcium channel Cav1.3 regulates insulin release and polymorphisms in CACNA1D associate with type 2 diabetes. Diabetologia *56*, 340–349.

Rezania, A., Bruin, J.E., Arora, P., Rubin, A., Batushansky, I., Asadi, A., O'Dwyer, S., Quiskamp, N., Mojibian, M., Albrecht, T., et al. (2014). Reversal of diabetes with insulin-producing cells derived in vitro from human pluripotent stem cells. Nat. Biotechnol. *32*, 1121–1133.

Rezania, A., Bruin, J.E., Riedel, M.J., Mojibian, M., Asadi, A., Xu, J., Gauvin, R., Narayan, K., Karanu, F., O'Neil, J.J., et al. (2012). Maturation of human embryonic stem cell-derived pancreatic progenitors into functional islets capable of treating pre-existing diabetes in mice. Diabetes *61*, 2016–2029.

Rezania, A., Bruin, J.E., Xu, J., Narayan, K., Fox, J.K., O'Neil, J.J., and Kieffer, T.J. (2013). Enrichment of human embryonic stem cell-derived NKX6.1-expressing pancreatic progenitor cells accelerates

the maturation of insulin-secreting cells in vivo. Stem Cells *31*, 2432–2442.

Russ, H.A., Parent, A.V., Ringler, J.J., Hennings, T.G., Nair, G.G., Shveygert, M., Guo, T., Puri, S., Haataja, L., Cirulli, V., et al. (2015). Controlled induction of human pancreatic progenitors produces functional beta-like cells in vitro. EMBO J. *34*, 1759–1772.

Sander, M., Sussel, L., Conners, J., Scheel, D., Kalamaras, J., Dela Cruz, F., Schwitzgebel, V., Hayes-Jordan, A., and German, M. (2000). Homeobox gene Nkx6.1 lies downstream of Nkx2.2 in the major pathway of beta-cell formation in the pancreas. Development *127*, 5533–5540.

Saxena, P., Heng, B.C., Bai, P., Folcher, M., Zulewski, H., and Fussenegger, M. (2016). A programmable synthetic lineage-control network that differentiates human IPSCs into glucose-sensitive insulin-secreting beta-like cells. Nat. Commun. *7*, 11247.

Song, S.H., Kjems, L., Ritzel, R., McIntyre, S.M., Johnson, M.L., Veldhuis, J.D., and Butler, P.C. (2002). Pulsatile insulin secretion by human pancreatic islets. J. Clin. Endocrinol. Metab. *87*, 213–221.

Song, S.H., McIntyre, S.S., Shah, H., Veldhuis, J.D., Hayes, P.C., and Butler, P.C. (2000). Direct measurement of pulsatile insulin secretion from the portal vein in human subjects. J. Clin. Endocrinol. Metab. *85*, 4491–4499.

Sussel, L., Kalamaras, J., Hartigan-O'Connor, D.J., Meneses, J.J., Pedersen, R.A., Rubenstein, J.L., and German, M.S. (1998). Mice lacking the homeodomain transcription factor Nkx2.2 have diabetes due to arrested differentiation of pancreatic beta cells. Development *125*, 2213–2221.

Takahashi, N., Hatakeyama, H., Okado, H., Noguchi, J., Ohno, M., and Kasai, H. (2010). SNARE conformational changes that prepare vesicles for exocytosis. Cell Metab. *12*, 19–29.

Tateishi, K., He, J., Taranova, O., Liang, G., D'Alessio, A.C., and Zhang, Y. (2008). Generation of insulin-secreting islet-like clusters from human skin fibroblasts. J. Biol. Chem. *283*, 31601–31607.

Terzic, A., and Behfar, A. (2016). Stem cell therapy for heart failure: Ensuring regenerative proficiency. Trends Cardiovasc. Med. *26*, 395–404.

Thatava, T., Kudva, Y.C., Edukulla, R., Squillace, K., De Lamo, J.G., Khan, Y.K., Sakuma, T., Ohmine, S., Terzic, A., and Ikeda, Y. (2013). Intrapatient variations in type 1 diabetes-specific iPS cell differentiation into insulin-producing cells. Mol. Ther. *21*, 228–239.

World Health Organization (2016). Global Report on Diabetes (World Health Organization). https://www.who.int/diabetes/global-report/en/.

Wijesekara, N., Dai, F.F., Hardy, A.B., Giglou, P.R., Bhattacharjee, A., Koshkin, V., Chimienti, F., Gaisano, H.Y., Rutter, G.A., and Wheeler, M.B. (2010). Beta cell-specific Znt8 deletion in mice causes marked defects in insulin processing, crystallisation and secretion. Diabetologia *53*, 1656–1668.

Yan-Do, R., Duong, E., Manning Fox, J.E., Dai, X., Suzuki, K., Khan, S., Bautista, A., Ferdaoussi, M., Lyon, J., Wu, X., et al. (2016). A glycine-insulin autocrine feedback loop enhances insulin secretion from human beta-cells and is impaired in type 2 diabetes. Diabetes *65*, 2311–2321.

Yang, S.Y., Lee, J.J., Lee, J.H., Lee, K., Oh, S.H., Lim, Y.M., Lee, M.S., and Lee, K.J. (2016). Secretagogin affects insulin secretion in pancreatic beta-cells by regulating actin dynamics and focal adhesion. Biochem. J. *473*, 1791–1803.

Yoshihara, E., Wei, Z., Lin, C.S., Fang, S., Ahmadian, M., Kida, Y., Tseng, T., Dai, Y., Yu, R.T., Liddle, C., et al. (2016). ERRgamma is required for the metabolic maturation of therapeutically functional glucose-responsive beta cells. Cell Metab. *23*, 622–634.

Zhu, Y., Liu, Q., Zhou, Z., and Ikeda, Y. (2017). PDX1, NEUROGENIN-3 and MAFA: critical transcription regulators for beta cell development and regeneration. Stem Cell Res. Ther. *8*, 240.

Stem Cell Reports, Volume *13*

Supplemental Information

Targeted Derivation of Organotypic Glucose- and GLP-1-Responsive β Cells Prior to Transplantation into Diabetic Recipients

Yaxi Zhu, Jason M. Tonne, Qian Liu, Claire A. Schreiber, Zhiguang Zhou, Kuntol Rakshit, Aleksey V. Matveyenko, Andre Terzic, Dennis Wigle, Yogish C. Kudva, and Yasuhiro Ikeda

Supplemental Figure S1. Zhu et al.

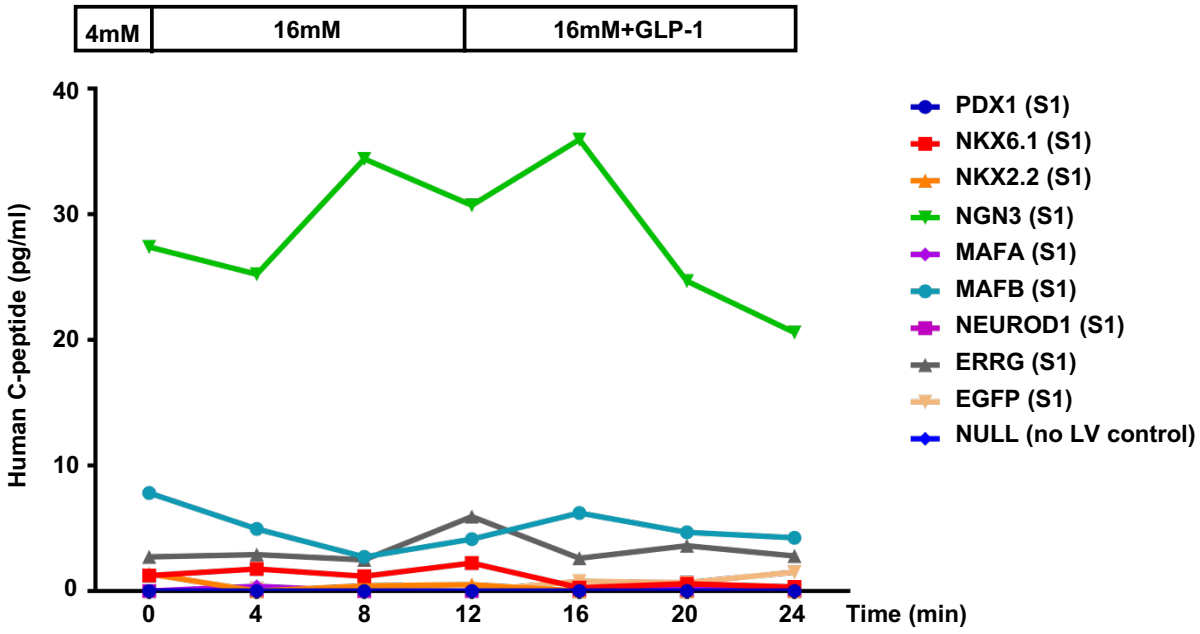

Figure S1. Secretion of human C-peptide by psBCs, Related to Fig.1e. Secretion of human C-peptide by psBCs in response to 4mM, 16mM and 16mM+GLP1 glucose medium for an indicated period of time. Different lentiviral vectors were introduced at the indicated stage.

Supplemental Figure S2. Zhu et al.

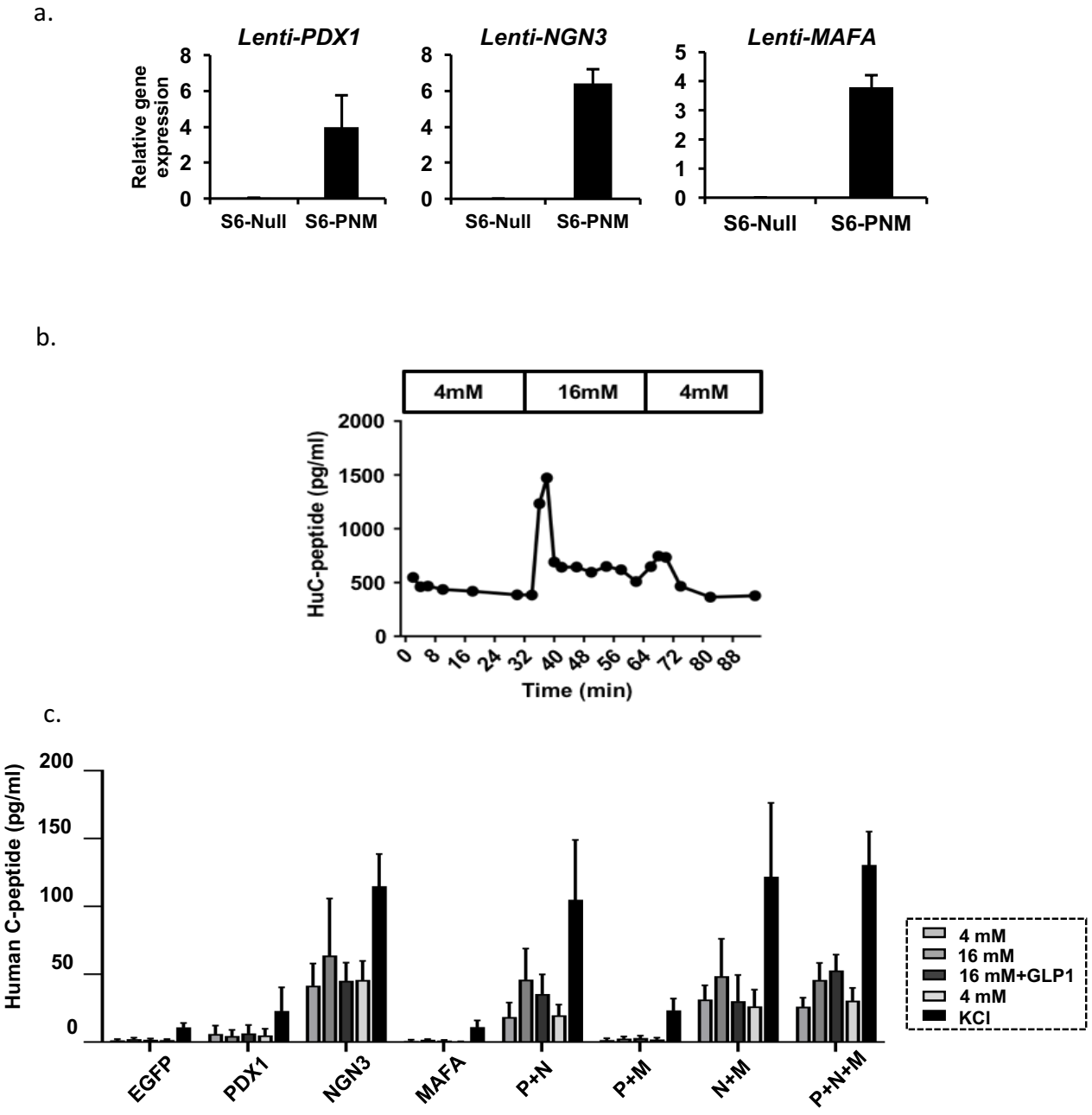

Figure S2. Glucose- and GLP-1-responsiveness of PNM-transduced psBCs, Related to Fig.2. (**a**) Levels of exogenous PDX1, NEUROG3 and MAFA gene expression in S6 psBCs were determined by qRT-PCR. (**b**) Secretion of human C-peptide by human islets in response to 4mM, 16mM and 4mM glucose medium for an indicated period of time. (**c**) Glucose- and GLP-1-responsive insulin secretion by psBCs transduced by different combinations of PNM factors. Levels of human C-peptide by psBCs in response to sequential 4mM, 16mM, 16mM+GLP-1, 4mM glucose medium and 30mM KCL incubation were analyzed by the perifusion system. Data represent the mean ± S.E.M. of the last time point of the first basal 4mM treatment, 4-minute time point for 16mM glucose treatment, 16mM glucose +GLP1 treatment, the second 4mM glucose treatment and KCL treatment.

Supplemental Figure S3. Zhu et al.

a.

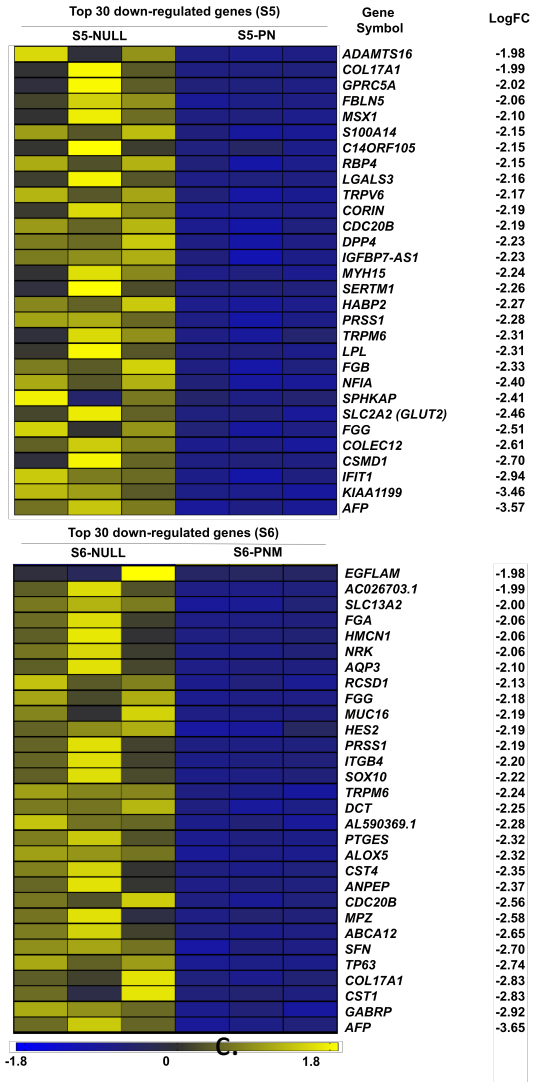

b.

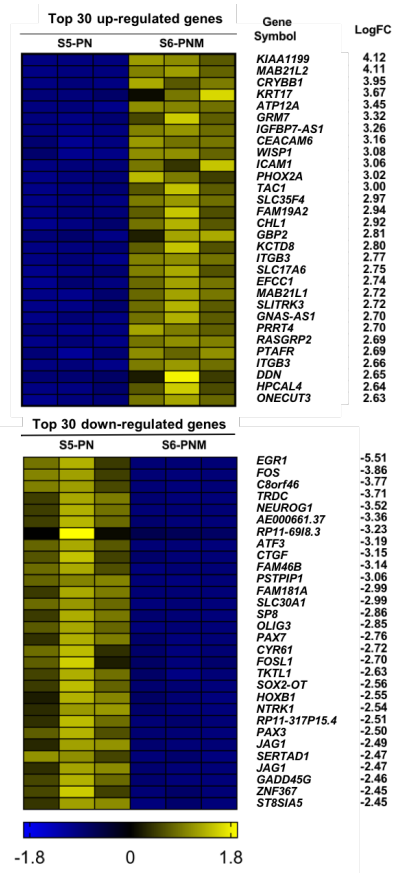

c.

	Gene Symbol	S6-PNM vs S5-PN (LogFC)
Beta cell & islet markers	*INS*	0.84
	CHGA	0.35
	CHGB	0.90*
	PDX1	-0.35
	NKX6.1	1.00*
	MAFB	-0.60*
	GLP1R	0.38
	GCGR	0.88*
	GCG	2.19*
	SST	0.21
GSIS-associated genes	*ADRA2A*	0.92*
	DOC2B	0.09
	ERRG	-0.36*
	GCK	0.93*
	MCT1	-0.44*
	MUNC18-1	0.70*
	MUNC18C	0.21
	PCSK1 (PC1)	1.54*
	PCSK2 (PC2)	0.47*
	PTPRN (IA-2)	0.98*
	SLC2A2 (GLUT2)	0.77
	SLC30A8 (ZnT8)	0.98*
	SLC6A5	2.25*
	SNAP25	1.25*
K^+/Ca^{2+} channel genes	*ABCC8*	0.91*
	ATP2B2	-0.18
	CACNA1D	0.80*
	CACNA2D3	1.70*
	KCNJ11	0.83*
	KCNK3	0.87*
	KCNQ1	0.51*
	MCU	-0.16*
	RYR2	-0.78
	SCGN	0.92*

d.

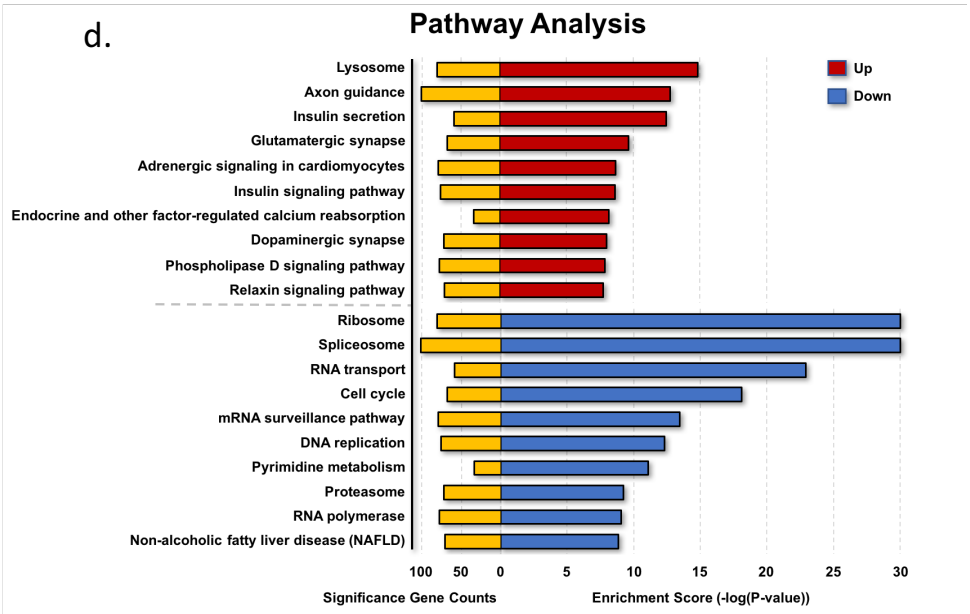

Figure S3. Characterization of PN and PNM transduced psBCs, Related to Fig.4. (**a**) Heatmaps of top 30 down-regulated genes for S5-PN and S6-PNM psBCs. LogFC stands for the $\log_2$ fold change of expression level relative to control. (**b**) Heatmaps of top 30 up-regulated and down-regulated genes for S6-PNM vs. S6-PN psBCs. LogFC stands for the $\log_2$ fold changes of expression level in S6-PNM psBCs relative to S5-PN psBCs. (**c**) Summary of differentially expressed genes between S5-PN and S6-PNM psBCs. LogFC stands for the $\log_2$ fold change of expression level of S6-PNM relative to S5-PN psBCs. **(d)** The top 10 up-regulated and down-regulated KEGG pathways of significantly differentially expressed genes between S5-PN and S6-PNM psBCs. KEGG, Kyoto Encyclopedia of Genes and Genomes. *represents statistically significant difference; Student's unpaired t-test.

Supplemental Figure S4. Zhu et al.

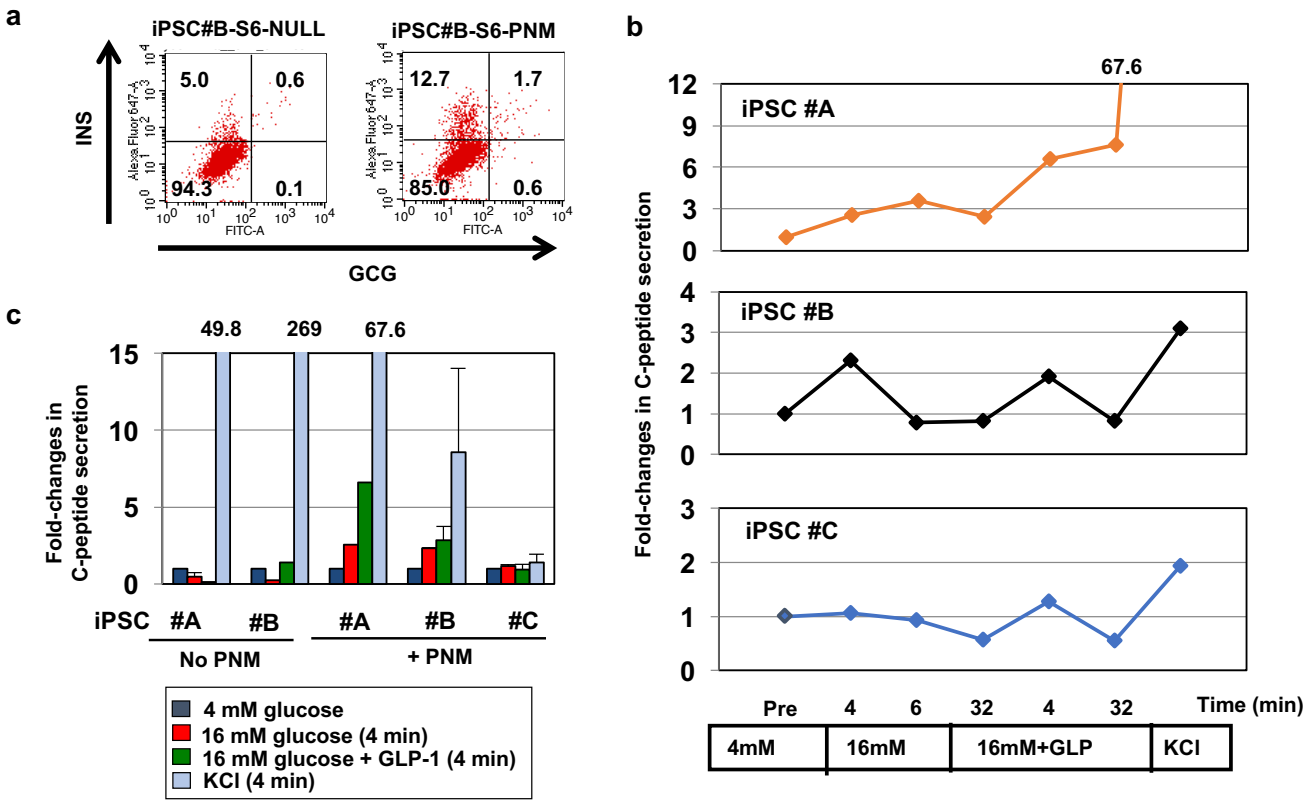

Figure S4. Effectiveness of PNM transduction in multiple iPSC lines, Related to Result 'PNM transduction in other iPSC lines'. We used five iPSC lines which were established by Sendai viral reprogramming and validated for their pluripotency and capacity to differentiate into insulin-positive cells (Kudva et al., Stem Cells Translational Medicine 2012). iPSC#A to #E were differentiated with or without PNM transduction and tested for their glucose and GLP-1 responsiveness by the perifusion system. (**a**) Same as Fig. 3b with iPSC#B. (**b**) Representative perifusion data of glucose- and GLP-1-responsiveness by iPSC clones #A, #B and #C. Experiments were performed the same way as Fig. 1e. (**c**) Summary of fold changes in C-peptide secretion, measured by perifusion. #C, #D and #E showed no notable glucose- and GLP-1-responsiveness (data not shown for #D and #E).

Supplemental Figure S5. Zhu et al.

a

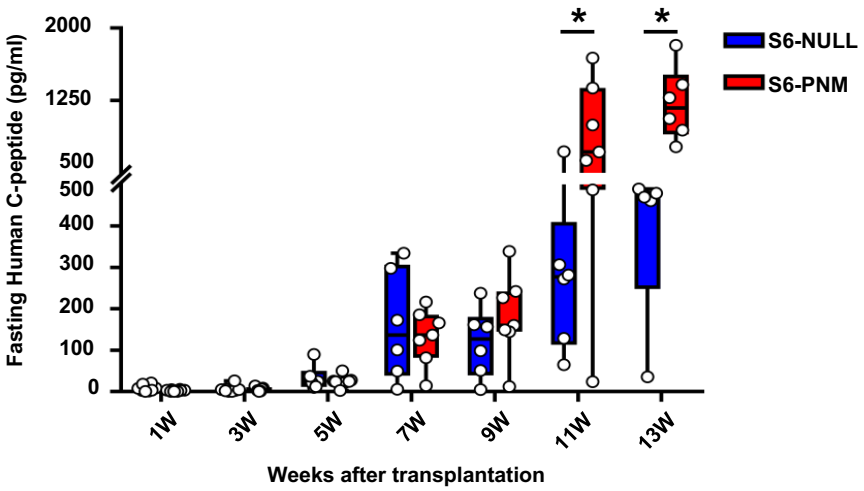

b

Figure S5. Characterization of psBCs *in vivo*, Related to Fig.5. (**a**) Fasting human C-peptide levels in mice that received S6-NULL and S6-PNM psBCs transplantation. C-peptide levels from individual mice are shown on box and whisker plots. Student's unpaired *t*-test. (**b**) IPGTT 7 weeks after transplantations in control mice (n=4), endoC cells transplanted mice (n=3), S6-Null transplanted mice (n=6), S6-PNM transplanted mice (n=7). Letter 'a' represents statistically significant difference between control and S6-PNM, letter 'b' represents difference between control and S6-NULL, letter 'c' represents difference between S6-NULL and S6-PNM, letter 'd' represents difference between control and beta cells, letter 'e' represents difference between S6-NULL and beta cells, letter 'f' represents difference between S6-PNM and beta cells; One-way ANOVA with Tukey test for multiple comparisons.

Table S1. Primer sequence used in this study, Related to Fig.4c.

Gene Name	FWD (5' to 3')	REV (5' to 3')
ABCC8	CGT CTT AGC TGT GCT TCT GT	CTT GGT CTG TAT TGC TCC TCT C
CACNA1D	GGG AGC AGG AGT ATT TCA GTA G	GAT GTT TCT GCC TGG GTA TCT
CACNA2D3	GAT GGC CTC CAA CTG GTA AA	CAT GTT TCA GGT GTG CTT CTT C
ESRRG	TCT CTA CCC TTC TGC TCC TAT C	GCA TCG AGT TGA GCA TGT ATT C
GAPDH	GCG CCC AAT ACG ACC AA	CTC TCT GCT CCT CCT GTT C
GCK	GAT GCA CTC AGA GAT GTA GTC G	TGA AGG TGG GAG AAG GTG AG
GLP1R	CTC CTT CTC TGC TCT GGT TAT C	CAG GTT CAG GTG GAT GTA GTT
INS	CTT CAC GAG CCC AGC CA	ATC AGA AGA GGC CAT CAA GC
KCNJ11	ATG AGG ACC ACA GCC TAC T	GGA ATC TGG AGA GAT GCT GAA C
PCSK1	CAG ACA GCA TCT ACA CCA TCT C	GTG TAA TCT CCG CTG CTG TAA
PCSK2	GAC CTG GCC TCC AAC TAT AAT G	TGT GTA CCG AGG GTA AGG ATA G
SLC30A8	GCA TGC CCT TGG AGA TCT ATT	GCA GAT TGG GTC GGC TAT TT
SLC6A5	GAA AGT CTG CTG GGC ATT TG	CAC CAT GGA CCA GTT AGG ATA G

METHODS

Cells. 293T cells were cultured in DMEM medium supplemented with 10% fetal calf serum and antibiotics. Commercially available iPSC lines IISH2i-BM9 (WiCell, Madison, Wisconsin), and in-house iPSC lines #A, #B, #C, #D and #E were tested for beta cell propensity. Undifferentiated iPSCs at passage 10-30 was cultured on Matrigel (Corning, Corning, NY, #354277) - coated plates in mTeSR1 medium (StemCell Technologies, Vancouver, Canada, #05850). Cultures were fed every day with mTeSR1 medium.

Lentiviral Vectors. Lentiviral vector genome plasmid, pSIN-CSGW-PKG-puro, which supports EGFP expression and puromycin selection, was kindly provided by Dr. Paul Lehner (Cambridge Institute for Medical Research). Codon-optimized ORF sequences for beta-cell factors, including PDX1, NEUROG3, NKX2.2, NKX6.1, NEUROD1, MAFA, MAFB and ESRRG, were designed and synthesized (GenScript, Piscataway, NJ), and cloned into the place of the EGFP gene in pSIN-CSGW-PKG-puro with the unique *Bam*HI and *Xho*I sites. Resulting vector plasmids were designated as pLenti-PDX1, pLenti-NEUROG3, pLenti-NKX2.2, pLenti-NKX6.1, pLenti-NEUROD1, pLenti-MAFA, pLenti-MAFB and pLenti-ESRRG, respectively. The internal spleen focus-forming virus (SFFV) promoter drives the expression of beta-cell factors. Lentiviral vectors were produced by plasmid transfection in 293T cells as described previously (Tonne and Campbell et al.,2011), concentrated by ultracentrifugation and re-suspended in phosphate buffered saline (PBS). Lentiviral titers were determined by puromycin selection.

Guided differentiation and stepwise lentiviral vector transduction. The basic differentiation strategy without viral vector transduction was a modified version of the previously published protocols. In pilot studies, we tested several reported differentiation protocols (Pagliuca and Millman et al.,2014,Rezania and Bruin et al.,2014) as well as the protocol we have been using, a modified Viacyte/Novocell protocol with additional Indolactam V for enhanced PDX1 expression (Thatava and Kudva et al.,2013,El Khatib and Ohmine et al.,2016). We also tested key ingredients targeting related pathways, including Wnt 3a vs GSK3b inhibitor, Activin A vs. GDF8, FGF10 vs. FGF7, Cyc vs. SANT1 (Shh inhibitors), and Indolactam V vs. TPB (PKC activators). Our final basic protocol was based on these pilot studies, which is similar to the Rezania's protocol(Rezania and Bruin et al.,2014), but with the use of Activin A and FCS instead of GDF8 and bovine serum albumin, and without heparin and the liquid-air interphase culture steps.
Guided differentiation was initiated 48 hours following seeding, with a 60-80% starting confluency with some spaces between iPSCs colonies. The basal medium was prepared by supplementing MCDB131 medium (Thermo Fisher Scientific, Waltham, MA, #10372019) with 1x Glutamax (Thermo Fisher Scientific, #35050061), 50 U/ml Penicillin, 50 µg/ml Streptomycin, 0.02% D-Glucose solution (45%, Sigma-Aldrich, St. Louis, MO, #G8769) and 2% Sodium Bicarbonate Solution (7.5%, Sigma-Aldrich, #S8761). Step 1 (S1, 3 days); Day 1 iPSCs were first rinsed with PBS without Mg2+ and Ca2+ and then cultured in the basal medium further supplemented with 0.5% FBS (Thermo, #A3160602), 100 ng/ml Activin A (R&D Systems, Minneapolis, MN, #338-AC-050) and 3 µM of CHIR-99021 (SelleckChem, Houston, TX, #S2924). Cells were cultured in 2 ml media each for a well of a 6-well-plate, 1 ml for a 12-well-plate. At day 2, culture supernatants were removed and cells were incubated with the basal medium with 0.5% FBS and 100 ng/ml Activin A. Cells were further infected with the Lenti-PDX1 vector once at an approximate MOI of 30 on day 2. For the screening of single lentiviral vectors for individual factors, each lentiviral vector was delivered at this time point. At day 3, culture supernatants were replaced by the basal medium with 0.5% FBS and 100 ng/ml Activin A. Step 2 (S2, 2 days); Cells were rinsed with PBS, then cultured with the basal medium 0.5% FBS, 0.25 mM ascorbic acid (Sigma-Aldrich, # A4544) and 50 ng/ml of FGF7 (R&D Systems, #251-KG-050). Culture supernatants were replaced with the same, fresh medium at day 2. Step 3 (S3, 2 days); The culture supernatants were replaced to the basal medium, further supplemented with 14 µl/ml of 7.5% sodium bicarbonate solution, 2% FBS, 0.25 mM ascorbic acid, 50 ng/ml FGF7, 0.25 µM SANT-1 (Sigma-Aldrich, # S4572), 1 µM retinoic acid (Sigma-Aldrich, #R2625), 100 nM LDN193189 (Stemgent, Lexington, MA, #04-0019), 1:200 ITS-X (Thermo Fisher Scientific, #51500056), and 100 nM alpha amyloid protein modulator (EMD Millipore, Billerica, MA, #565740). Medium was changed every day. Step 4 (S4, 3 days); The culture supernatants of S3 cells were replaced with the basal medium further supplemented with 14 µl/ml of 7.5% sodium bicarbonate solution, 2% FBS, 0.25 mM ascorbic acid, 2 ng/ml of FGF7, 0.25 µM SANT-1, 0.1 µM retinoic acid, 200 nM LDN193189, 1:200 ITS-X, and 100 nM TPB. Cells were also infected with the Lenti-NEUROG3 vector at an approximate MOI of 30 once on day 7 (end of Step 3) or day 8 (beginning of Step 4). Medium changed every day with the fresh media. Step 5 (S5, 3 days); Cells were cultured in the basal medium further supplemented with 14 µl/ml of 7.5% sodium bicarbonate solution, 4 µl/ml of 45% glucose solution, 2% FBS, 0.25 µM SANT-1, 10 µM ALK5 inhibitor II (Enzo Life Sciences, Farmingdale, New York, #ALX-270-445), 0.05 µM retinoic acid, 1 µM thyroid hormone (Sigma-Aldrich, #T6397), 100 nM LDN193189, 1:200 ITS-X, 10 µM zinc sulfate (Sigma-Aldrich, #Z0251) and 10 µg/ml heparin (Sigma-Aldrich, #H3149). Medium was replaced every day. Step 6 (S6, 7 days); Culture media were replaced with the basal medium further supplemented with 14 µl/ml of 7.5% sodium bicarbonate solution, 4 µl/ml of 45% glucose solution, 2% FBS, 1 µM thyroid hormone, 10 µM ALK5 inhibitor II, 10 µM zinc sulfate, 100nM LDN193189, 1:200 ITS-X, 10 µg/ml heparin, and 100 nM gamma secretase inhibitor XX (EMD Millipore, Billerica, MA, # 565789) for 7 days. Cells were also infected with the Lenti-MAFA vector at an approximate MOI of 30 once, on day 14, 15, or 16. Fresh medium was fed every day.

qRT-PCR. For quantitative reverse transcription polymerase chain reaction (qRT-PCR), total RNA from differentiated iPSCs at indicated time points was isolated using Trizol according to the manufacturer instructions. cDNAs were then synthesized by reverse transcription from 200 ng of total RNA using SuperScript III Reverse Transcriptase, dNTP solutions, RNaseOUT and Random Hexamer. Hotstart Taq DNA polymerase and primer pairs for human *INS, GCK, GLP1R, ESRRG, SLC6A5, SLC30A8, ABCC8, KCNJ11, CACNA1D, CACNA2D3, PCSK1* and *PCSK2* were used. Sequence of the primers used for qRT–PCR was listed in Table S1. The PCR conditions were 95°C for 10 minutes enzyme activation, 95°C for 15 seconds denaturation, 60°C for 60 seconds annealing and extension, and overall 40 cycles were performed. The transcript levels were normalized to glyceraldehyde 3-phosphate dehydrogenase (GAPDH).

RNA sequencing. For RNA sequencing, a total 200 ng RNA from differentiated iPSCs at indicated time points was isolated using RNeasy Mini Kit. Library preparation (TruSeq mRNA v2 (TMRNA)) and next-generation sequencing and analysis (standard secondary analysis pipeline, MAPRSeq) were performed in Mayo Clinic Sequencing and Bioinformatics Cores. Heatmap was depicted using Graphpad Prism.

Immunofluorescence staining. Lentiviral vector-infected 293T cells were fixed with 4% paraformaldehyde (PFA) for 20 min. After fixation cells were washed once with PBS and were then permeabilized with 0.3% Triton X-100 in PBS for 10 min. Cells were then washed with PBS twice and were blocked with 5% FBS in PBS for 1 hours. Cells were incubated overnight with rabbit anti-human PDX1 (1:200, Abcam, Cambridge, MA, #AB47267), rabbit anti-human NEUROG3 (1:50, DSHB, Iowa City, IA, #F25A1B3), rabbit anti-human MAFA (1:200, Abcam, #AB47267), goat anti-human NKX6.1 (1:100, R&D Systems, #AF5857), rabbit anti-human NEUROD1(1:200, Sigma, #N3663), mouse anti-human NKX2.2 (1:50, DSHB, #74.5A5), anti-human ESRRG (1:100, Abcam, #AB131593), mouse anti-human MAFB (1:25, R&D Systems, #MAB3810) overnight at 4°C, followed by incubation with secondary antibodies for 1 hour at room temperature.
For the characterization of psBCs, undifferentiated iPSCs were seeded on chamber slides and went through the differentiation protocol described above. Differentiated cells were fixed at the indicated time points and were permeabilized and blocked as described above. Cells were incubated overnight with guinea pig anti-human insulin (1:400, Dako, Santa Clara, CA, # A056401), goat anti-human NKX6.1 (1:100), rabbit anti-human NEUROD1(1:200), mouse anti-human NKX2.2 (1:50), mouse anti-human glucagon (1:300, Abcam, #ab10988-100), rabbit anti-human somatostatin (1:100, Santa Cruz, Dallas, Texas, #sc-20999) or mouse anti-human C-peptide (1:400, Thermo Fisher Scientific, #MA1-19159) overnight at 4°, followed by incubation with secondary antibodies for 1 hour at room temperature. Nuclei were counterstained by DAPI (blue)
Mouse Kidneys with the grafts were harvested and frozen in OCT Compound. 7 μm pancreatic cryosections were immediately fixed, permeabilized and then blocked as described above .Slides were then incubated with guinea pig anti-human insulin (1:400), goat anti-human NKX6.1 (1:100), rabbit anti-human NEUROD1 (1:200), mouse anti-human NKX2.2 (1:50), mouse anti-human glucagon (1:300), rabbit anti-human somatostatin (1:100) overnight at 4°, followed by secondary antibody incubation for 1 hour at room temperature. Nuclei were counterstained by DAPI (blue). Images were taken using a Zeiss LSM 780 confocal laser scanning microscope and analyzed with Zeiss imaging software. Fluorescence intensity were analyzed by Image J software.

Flow cytometry. iPSC-derived psBCs were dispersed into single-cell suspension by incubation in Trypsin at 37°C for 10 minutes, quenched with 3-4 volumes of FCS-containing culture media and cells were spun down for 5 min at 800g. Cells were transferred to a 1.7ml microcentrifuge tube, fixed in 4%PFA, permeabilized with 0.3% Triton-X and then blocked with 5% FBS for 1 hours. Cells were incubated overnight with guinea pig anti-human insulin (1:400), mouse anti-human glucagon (1:300), mouse anti-human C-peptide (1:400) at 4°C. After washing three times with 5% FBS, cells were stained with secondary antibodies. Cell were then washed and filtered through a 35μm mesh Falcon tube, and analyzed using the LSR-II flow cytometer (BD Biosciences). Analysis of the results was performed using FlowJo software.

Electron microscopy. iPSC-derived psBCs were fixed at room temperature. Cell samples were processed and analyzed by transmission Electron Microscopy at Mayo Clinic Microscopy and Cell Analysis Core.

***In vitro* GSIS assay.** We used an islet perifusion system (Biorep technologies, Miami Lakes, FL). Approximately 1 x 106 psBCs differentiated in wells of 48-well plates, or cadaver human islets (n=200 hand-picked islets) were first incubated in 4mM glucose Krebs Ringer Bicarbonate buffer supplemented with 0.2% BSA for 30 minutes at 37°C. Cells were then gently scraped off from the wells, transferred into a sterile 1.5ml eppendorf tube, and centrifuged at 37°C for 5 minutes. Cell pellets were transferred into the perifusion chamber and were washed for 40 minutes in the perifusion system with 4mM glucose buffer, which were preheated to 37°C and oxygenized with 95% O2 and 5% CO2. After washing, cells were exposed to 4mM glucose perifusate for 32min, followed by 32 minutes of 16mM glucose buffer, 32 minutes of 16mM glucose buffer supplemented with 100nM GLP-1 (Peprotech, Rocky Hill, NJ, #130-08-1MG), 32 minutes of 4mM glucose buffer and finally 8 minutes of 16mM glucose buffer supplemented with 30mM KCL. Effluent was collected in 2-minute intervals and assayed for human C-peptide by ELISA (Alpco, Salem, NH, #80-CPTHU-CH01) for subsequent determination of basal and GSIS.

Mice transplantation studies. All animal experiments were performed in accordance with Mayo Clinic International Animal Care and Use Committee (IACUC) regulations. Immunodeficient Fox Chase SCID-Beige mice, aged 8-10 weeks, were purchased from Charles River Laboratory. To induce diabetes, mice received 50 mg/kg body weight streptozotocin (STZ, Sigma, #S0130) intraperitoneally over the course of five consecutive days. Mice with non-fasting blood glucose levels over 250 mg/dl after STZ administration were used and randomized into four groups in the following experiments. PsBCs clusters (approximately 50 million cells per mouse), and human beta-cell line (EndoC-βH2 cells, approximately 5 million cells per mouse) were gently scraped off and transferred into a 15ml conical vial. After spinning for 5 minutes at 800g, cells were loaded into a catheter for cell delivery into the kidney capsules (El Khatib and Sakuma et al.,2015). 1 day, 4 day and 1, 2, 3, 5, 7, 9, 11, 13 weeks after the surgery, fasting (16 hours) blood glucose was tested using glucose monitor and strips. To measure glucose-responsive C-peptide secretion, fasting blood and 30 minutes blood after an intraperitoneal injection of D-(+)-glucose at 2g/kg body weight was collected through retro orbital bleeding every two weeks. Serum was separated out using Microvettes (Sarstedt, Nümbrecht, Germany, #20.1278.100) and stored at 80°C until ELISA analysis. At indicated time points, kidneys containing the grafts were dissected from the mice, embedded and frozen in OCT compound. Immunostaining was performed as described above. No statistical method was used for sample size estimation. Investigators were not blinded to the group allocations. Mice transplantation study was performed in duplicate.

Intraperitoneal glucose tolerance test (IPGTT). To measure glucose handling capacity *in vivo*, mice were fasted (16 hours) and blood glucose was tested at 0min, 30min, 60min, 90min, 120min after IP injection of D-(+)-glucose at 2g/kg body weight.

Sample size and statistical analysis. All data represent the means ±S.E.M. of three to nine samples, as indicated in the figure legends. Group comparisons were analyzed by unpaired or paired *t* tests, one sample *t* test and one-way ANOVA with Tukey test through IBM SPSS Statistics 22. *P<0.05, **P<0.01, ***P<0.001. Bar graphs, heatmaps, curves, box and whisker plots were generated with GraphPad Prism7 and Excel 2010.